

Simulator of photoemission angular distribution for experiments (SPADExp)

Hiroaki Tanaka (ISSP / Graduate School of Science, The Univ. of Tokyo)

October 31, 2022

Contents

1	Calculation theory	5
1.1	Hartree-Fock-Slater equation	6
1.1.1	Atomic units	6
1.1.2	Exchange-correlation terms in free electron gas	6
1.1.3	HFS equation	8
1.1.4	Thomas-Fermi potential	8
1.2	Calculations of atomic potentials	10
1.2.1	Numerical solutions of differential equations	10
1.2.2	Calculations of the Thomas-Fermi potential	11
1.2.3	Schrödiger equation in an isotropic potential	12
1.2.4	Calculations of self-consistent atomic potentials	14
1.3	Special functions for radial wave functions	16
1.3.1	Gamma functions	16
1.3.2	Bessel functions, spherical Bessel functions	17
1.3.3	Coulomb wave functions	22
1.3.4	Spherical harmonics	25
1.3.5	Partial wave expansion	28
1.4	Photoemission angular distribution calculations	30
1.4.1	Overview	30
1.4.2	Initial states	30
1.4.3	Final States	30
1.4.4	Perturbation term	30
2	Software	33
2.1	Atomic and pseudo-atomic orbitals in OpenMX and ADPACK	34
2.1.1	Modification of ADPACK	34
2.1.2	Comparison of orbitals	34
2.2	GUI_tools directory	37
2.2.1	Overview	37
2.2.2	OpenMX_viewer	37
2.2.3	OpenMX_orbitals	38
2.2.4	OpenMX_band	38
2.3	OpenMX_tools directory	39
2.3.1	Compilation	39
2.3.2	preproc.o	39
2.3.3	postproc.o	40
2.4	SPAExp_GUI tools	41
2.4.1	SPAExp_GUI	41
2.4.2	SPAExp_Viewer	41
2.5	Main_program directory	43
2.5.1	Compilation	43
2.5.2	Overview	43
2.5.3	&Control block	43
2.5.4	Calculation of the Thomas-Fermi potential	43
2.5.5	Calculations of atomic wave functions	44
2.5.6	Calculations of the self-consistent atomic potential	46

2.5.7	Calculations of excited states and phase shifts	47
2.5.8	Photoemission intensity calculations	48

Chapter 1

Calculation theory

1.1 Hartree-Fock-Slater equation

Plane waves for photoelectron wave functions are modified by atomic potentials. Here, we explain Hartree-Fock-Slater (HFS) equations to obtain self-consistent atomic potentials.

1.1.1 Atomic units

The following arguments use **the atomic unit**, in which the following physical constants are omitted.

- **Electron mass** $m = 9.109 \times 10^{-31}$ kg
- **Bohr radius** $a_0 = 0.5292$ Å
- **Elementary charge** $e = 1.602 \times 10^{-19}$ C
- **Dirac constant** $\hbar = 1.054 \times 10^{-34}$ J · s

Values in the SI unit is from Ref. [1]. Therefore, the units of energy and wavevector become $E_h = 27.2114$ eV and $1/a_0 = 1.890$ Å⁻¹, respectively. Since Ref. [2] uses Ryberg ($E_h/2$) as the unit, coefficients may be different twice.

1.1.2 Exchange-correlation terms in free electron gas

In the HFS equations, the exchange-correlation term is approximated by the local density approximation (LDA). Here we calculate the term in free electron gas with number density n .

In a three-dimensional space with large enough volume V , wavefunctions of free-electron gases $\psi_{\mathbf{k}}(\mathbf{r})$ and eigenenergies $E(\mathbf{k})$ become

$$\psi_{\mathbf{k}}(\mathbf{r}) = \frac{1}{\sqrt{V}} e^{i\mathbf{k} \cdot \mathbf{r}}, \quad E(\mathbf{k}) = \frac{1}{2} |\mathbf{k}|^2. \quad (1.1)$$

We represent the Fermi wavevector by k_F , and using that the number density coefficient in the reciprocal space is $1/(2\pi)^3$, we obtain the following relationship;

$$n = 2 \times \frac{4}{3} \pi k_F^3 \cdot \frac{1}{(2\pi)^3} = \frac{k_F^3}{3\pi^2}. \quad (1.2)$$

We solve the above equation w.r.t. k_F , and then get

$$k_F = (3\pi^2 n)^{1/3}. \quad (1.3)$$

We calculate the exchange-correlation term where $|\mathbf{k}| < k_F$ region is occupied by the Hartree-Fock approximation. Here we calculate the term for only one spin direction.

$$E_{xc} = -\frac{1}{2} \sum_{i,j} \int d^3\mathbf{r}_1 d^3\mathbf{r}_2 \psi_i^*(\mathbf{r}_1) \psi_j^*(\mathbf{r}_2) \frac{1}{|\mathbf{r}_1 - \mathbf{r}_2|} \psi_j(\mathbf{r}_1) \psi_i(\mathbf{r}_2) \quad (1.4)$$

$$= -\frac{1}{2V^2} \sum_{i,j} \int d^3\mathbf{r}_1 d^3\mathbf{r}_2 \frac{1}{|\mathbf{r}_1 - \mathbf{r}_2|} e^{i(\mathbf{k}_j - \mathbf{k}_i) \cdot (\mathbf{r}_1 - \mathbf{r}_2)} \quad (1.5)$$

using $\mathbf{r}_3 = \mathbf{r}_1 - \mathbf{r}_2$ as a new integral variable,

$$= -\frac{1}{2V} \sum_{i,j} \int d^3\mathbf{r}_3 \frac{1}{|\mathbf{r}_3|} e^{i(\mathbf{k}_j - \mathbf{k}_i) \cdot \mathbf{r}_3} \quad (1.6)$$

in the polar coordinate system with principal axis parallel to $\mathbf{k}_j - \mathbf{k}_i$,

$$= -\frac{1}{2V} \sum_{i,j} \int_0^\infty r_3^2 dr_3 \int_0^\pi \sin \theta d\theta \int_0^{2\pi} d\varphi \frac{1}{r_3} e^{iKr_3 \cos \theta} \quad (K = |\mathbf{k}_j - \mathbf{k}_i|) \quad (1.7)$$

$$= -\sum_{i,j} \frac{\pi}{iKV} \int_0^\infty (e^{iKr_3} - e^{-iKr_3}) dr_3 \quad (1.8)$$

Adding a convergence factor $e^{-\eta r}$, finally we get

$$= - \sum_{i, j} \frac{2\pi}{K^2 V}. \quad (1.9)$$

Next, we calculate the sum w.r.t. \mathbf{k}_j with fixed \mathbf{k}_i ,

$$E_{\text{xc}} = -\frac{2\pi}{V} \sum_i \int_{|\mathbf{k}_j| < k_F} d^3 \mathbf{k}_j \frac{1}{K^2} \cdot \frac{V}{(2\pi)^3} \quad (1.10)$$

in polar coordinate system with principal axis parallel to \mathbf{k}_i ,

$$= -\frac{1}{4\pi^2} \sum_i \int_0^{k_F} k_j^2 dk_j \int_0^\pi \sin \theta d\theta \int_0^{2\pi} d\varphi \frac{1}{k_i^2 + k_j^2 - 2k_i k_j \cos \theta} \quad (k_i = |\mathbf{k}_i|, k_j = |\mathbf{k}_j|) \quad (1.11)$$

$$= -\frac{1}{2\pi} \sum_i \frac{1}{k_i} \int_0^{k_F} dk_j k_j \left(\log |k_i + k_j| - \log |k_i - k_j| \right) \quad (1.12)$$

Using

$$\int_0^b x \log |x + a| dx = \left[\frac{1}{2} x^2 \log |x + a| - \frac{1}{4} x^2 + \frac{a}{2} x - \frac{a^2}{2} \log |x + a| \right]_0^b \quad (1.13)$$

$$= \frac{b^2 - a^2}{2} \log |b + a| - \frac{1}{4} b^2 + \frac{ab}{2} + \frac{a^2}{2} \log |a|, \quad (1.14)$$

we get

$$E_{\text{xc}} = -\frac{1}{2\pi} \sum_i \frac{1}{k_i} \left[\frac{k_F^2 - k_i^2}{1} (\log |k_F + k_i| - \log |k_F - k_i|) + k_F k_i \right] \quad (1.15)$$

$$= -\frac{k_F}{2\pi} \sum_i \left(1 + \frac{k_F^2 - k_i^2}{2k_F k_i} \log \left| \frac{k_i + k_F}{k_i - k_F} \right| \right). \quad (1.16)$$

At last we take the summation w.r.t \mathbf{k}_i ,

$$E_{\text{xc}} = -2k_F \int_0^{k_F} k_i^2 dk_i \left(1 + \frac{k_F^2 - k_i^2}{2k_F k_i} \log \left| \frac{k_i + k_F}{k_i - k_F} \right| \right) \cdot \frac{V}{(2\pi)^3} \quad (1.17)$$

$$= -\frac{k_F^4 V}{12\pi^3} + \frac{V}{8\pi^3} \int_0^{k_F} dk_i k_i (k_i^2 - k_F^2) (\log |k_i + k_F| - \log |k_i - k_F|) \quad (1.18)$$

Using

$$\int_0^b x(x^2 - a^2) \log |x + a| dx = \left[\left(\frac{1}{4} x^4 - \frac{a^2}{2} x^2 \right) \log |x + a| - \frac{1}{16} x^4 + \frac{a}{12} x^3 + \frac{a^2}{8} x^2 - \frac{a^3}{4} x + \frac{a^4}{4} \log |x + a| \right]_0^b \quad (1.19)$$

$$= \frac{(b^2 - a^2)^2}{4} \log |b + a| + \frac{1}{48} (-3b^4 + 4ab^3 + 6a^2b^2 - 12a^3b) - \frac{a^4}{4} \log |a|, \quad (1.20)$$

we get

$$E_{\text{xc}} = -\frac{k_F^4 V}{12\pi^3} - \frac{k_F^4 V}{24\pi^3} = -\frac{k_F^4 V}{8\pi^3}. \quad (1.21)$$

Electron with the other spin has the same energy, so the exchange-correlation term per one electron becomes

$$e_{\text{xc}} = 2E_{\text{xc}} \times \frac{1}{nV} = -\frac{3k_F}{4\pi}. \quad (1.22)$$

The exchange-correlation potential becomes twice because the energy is half to avoid double counting. Therefore, the exchange-correlation potential in the LDA approximation is

$$V_{\text{xc}} = 2e_{\text{xc}} = -3 \left(\frac{3n}{8\pi} \right)^{1/3}. \quad (1.23)$$

1.1.3 HFS equation

The HFS equation is obtained by averaging the Hartree-Fock equation along the angle direction. Since the potential becomes spherically isotropic, the wavefunctions can be separated by radial functions and spherical harmonics;

$$\psi(\mathbf{r}) = \frac{P_{nl}(r)}{r} Y_{lm}(\theta, \varphi). \quad (1.24)$$

Here, the HFS equation of $P_{nl}(r)$ becomes

$$\left[-\frac{1}{2} \frac{d^2}{dr^2} + \frac{l(l+1)}{2r^2} + V(r) \right] P_{nl}(r) = E_{nl} P_{nl}(r). \quad (1.25)$$

The potential $V(r)$ is the sum of nucleus potential, Hartree term, and Fock term;

$$V(r) = -\frac{Z}{r} + \frac{1}{r} \int_0^r \sigma(r') dr' + \int_r^\infty \frac{\sigma(r')}{r'} dr' - 3 \left(\frac{3\rho(r)}{8\pi} \right)^{1/3} \quad (1.26)$$

$$\sigma(r) = \sum_{nl} w_{nl} (P_{nl}(r))^2 \quad (1.27)$$

$$\rho(r) = \frac{\sigma(r)}{4\pi r^2}, \quad (1.28)$$

where w_{nl} is the occupation number of each orbital, Z is the atomic number. There are given as input paramters. $\sigma(r)$ is the number density integrated along the angle direction, and $\rho(r)$ is the number density per unit volume. When the atomic potential $V(r)$ becomes self-consistent, that potential is the solution.

1.1.4 Thomas-Fermi potential

When we try to obtain self-consistent potential in the HFS equation, the initial potential is given by the Thomas-Fermi potential [22]. We put the atomic nucleus with charge Z at the coordinate origin, and consider Z electrons around it. We represent the potential and electron density by $V(r)$ and $\rho(r)$, respectively. Also, we suppose the relationship electron gases $\rho(r) = k_F(r)^3/3\pi^2$ similar to electron gases.

The Fermi level, determined by the potential and Fermi wavevector, should be isotropically uniform, so the relationship

$$E_F = \frac{1}{2} k_F(r)^2 + V(r) = \text{const.} = 0 \quad (1.29)$$

hold. We represent k_F as a function of $\rho(r)$, and using $V(r) = -\phi(r)$ where $\phi(r)$ is the electric field, then we get

$$E_F = \frac{1}{2} (3\pi^2 \rho(r))^{2/3} - \phi(r). \quad (1.30)$$

Combining it with the Poisson equation of the electric field

$$\Delta\phi(r) = 4\pi\rho(r) \quad (\rho(r) \text{ is the number density of electrons}), \quad (1.31)$$

then we get

$$\frac{1}{r^2} \frac{d}{dr} r^2 \frac{d}{dr} (\phi(r) + E_F) = \frac{4}{3\pi} (2(\phi(r) + E_F))^{3/2}. \quad (1.32)$$

We define a function $f(r)$ by

$$f(r) = \frac{r}{Z} (\phi(r) + E_F). \quad (1.33)$$

In the limit $r \rightarrow 0$, $\phi(r) \rightarrow Z/r$ should be dominant, so $f(r) \rightarrow 1$. On the other hand, in the limit $r \rightarrow \infty$ electron density and the potential becomes zero so $f(r) \rightarrow 0$. Using $f(r)$, we get

$$\frac{1}{r} \frac{d^2}{dr^2} f(r) = \frac{4}{3\pi} r^{-3/2} Z^{1/2} (2f(r))^{3/2} \quad (1.34)$$

$$\iff \frac{d^2}{dr^2} f(r) = \frac{2^{7/2} Z^{1/2}}{3\pi} \frac{1}{r^{1/2}} f(r)^{3/2}. \quad (1.35)$$

To obtain simple coefficients by the scaling $r = \mu x$, using $g(x) = f(r) = f(\mu x)$ we get

$$\frac{1}{\mu^2} \frac{d^2}{dx^2} g(x) = \frac{2^{7/2} Z^{1/2}}{3\pi} \frac{1}{(\mu x)^{1/2}} g(x)^{3/2} \quad (1.36)$$

$$\frac{d^2}{dx^2} g(x) = \frac{2^{7/2} Z^{1/2}}{3\pi} \frac{\mu^{3/2}}{x^{1/2}} g(x)^{3/2} \quad \therefore \mu = \left(\frac{3\pi}{2^{7/2} Z^{1/2}} \right)^{2/3} = \frac{1}{2Z^{1/3}} \left(\frac{3\pi}{4} \right)^{2/3}. \quad (1.37)$$

Using this scaling, the equation to solve becomes

$$\frac{d^2}{dx^2} g(x) = \frac{g(x)^{3/2}}{\sqrt{x}}, \quad (1.38)$$

and the Thomas-Fermi potential is obtained by the following equation;

$$V(r) = -\frac{Z}{r} g(r/\mu), \quad V(\mu x) = -\frac{Z}{\mu x} g(x). \quad (1.39)$$

1.2 Calculations of atomic potentials

We explain the process to numerically calculate atomic potentials based on Hartree-Fock-Slater (HFS) equations.

1.2.1 Numerical solutions of differential equations

Reduction to first-order differential equations

The differential equations in the following discussions can be represented by the form of

$$\frac{d^2}{dx^2} f(x) = F(f(x), x) \quad (1.40)$$

and are solved in $x \geq 0$ region. Some of them satisfy the relationship $F(f(x), x) = -a(x) \cdot f(x)$ ¹. Using $f'(x) = \frac{d}{dx} f(x)$, we can transform the equations to a first-order differential equation like

$$\frac{d}{dx} \begin{pmatrix} f(x) \\ f'(x) \end{pmatrix} = \begin{pmatrix} f'(x) \\ F(f(x), x) \end{pmatrix}. \quad (1.41)$$

Euler method

Euler method calculates the value at x_{i+1} using only the value at x_i . We take a sequence of points x_i ($i = 0, 1, \dots$) in $x \geq 0$ region satisfying $0 = x_0 < x_1 < \dots < x_i < x_{i+1} < \dots$; the distances between two adjacent points $x_{i+1} - x_i$ need not to be uniform. Also, we suppose that the initial values $f(0)$, $f'(0)$ are given. In this situation, the values at x_{i+1} , $f(x_{i+1})$ and $f'(x_{i+1})$ can be calculated from those at x_i by the following equations;

$$f(x_{i+1}) = f(x_i) + f'(x_i)(x_{i+1} - x_i) \quad (1.42)$$

$$f'(x_{i+1}) = f'(x_i) + F(f(x_i), x_i)(x_{i+1} - x_i). \quad (1.43)$$

Although Euler method is less precise than following methods because the error is proportional to the step width [4], it is more general because it does not require an equally-separated grid.

4th-order Runge-Kutta method

First we describe the general form of 4th-order Runge-Kutta method. We suppose a first-order differential equation of a vertical vector $\mathbf{y}(x)$ like

$$\frac{d}{dx} \mathbf{y}(x) = \mathbf{f}(\mathbf{y}(x), x), \quad (1.44)$$

where $\mathbf{f}(\mathbf{y}(x), x)$ is a function which returns a vertical vector of the same dimension as $\mathbf{y}(x)$. Using sequence of points x_i equally-separated with the distance h , \mathbf{y}_{i+1} can be calculated by

$$\mathbf{k}_1 = \mathbf{f}(\mathbf{y}(x_i), x_i) \quad (1.45)$$

$$\mathbf{k}_2 = \mathbf{f}(\mathbf{y}(x_i) + h\mathbf{k}_1/2, x_i + h/2) \quad (1.46)$$

$$\mathbf{k}_3 = \mathbf{f}(\mathbf{y}(x_i) + h\mathbf{k}_2/2, x_i + h/2) \quad (1.47)$$

$$\mathbf{k}_4 = \mathbf{f}(\mathbf{y}(x_i) + h\mathbf{k}_3, x_i + h) \quad (1.48)$$

$$\mathbf{y}_{i+1} = \mathbf{y}_i + h \left[\frac{1}{6}\mathbf{k}_1 + \frac{1}{3}\mathbf{k}_2 + \frac{1}{3}\mathbf{k}_3 + \frac{1}{6}\mathbf{k}_4 \right]. \quad (1.49)$$

This method gives the error proportional to the 4th power of the step h [4].

In our situation, 4th-order Runge-Kutta method becomes

$$k_1 = f'(x_i) \quad k'_1 = F(f(x_i), x_i) \quad (1.50)$$

$$k_2 = f'(x_i) + hk'_1/2 \quad k'_2 = F(f(x_i) + hk_1/2, x_i + h/2) \quad (1.51)$$

$$k_3 = f'(x_i) + hk'_2/2 \quad k'_3 = F(f(x_i) + hk_2/2, x_i + h/2) \quad (1.52)$$

$$k_4 = f'(x_i) + hk'_3 \quad k'_4 = F(f(x_i) + hk_3, x_i + h) \quad (1.53)$$

$$f(x_{i+1}) = f(x_i) + h \left[\frac{1}{6}k_1 + \frac{1}{3}k_2 + \frac{1}{3}k_3 + \frac{1}{6}k_4 \right] \quad f'(x_{i+1}) = f'(x_i) + h \left[\frac{1}{6}k'_1 + \frac{1}{3}k'_2 + \frac{1}{3}k'_3 + \frac{1}{6}k'_4 \right]. \quad (1.54)$$

¹The minus sign is to match the Numerow method.

Numerov method

Numerov can be used if the differential equation satisfies $F(f(x), x) = -a(x) \cdot f(x)$. We do not use a simultaneous differential equation form like above, but we calculate the value by the following equation;

$$f(x_{i+1}) = \frac{2(1 - 5h^2a(x_i)/12)f(x_i) - (1 + h^2a(x_{i-1})/12)f(x_{i-1})}{1 + h^2a(x_{i+1})/12}, \quad (1.55)$$

where h is the distance between two adjacent points and must be constant.

The above equation is derived as follows[4]. First, using Störmer's formula

$$f(x_{i+1}) - 2f(x_i) + f(x_{i-1}) = \frac{h^2}{12} \left(F(f(x_{i+1}), x_{i+1}) + 10F(f(x_i), x_i) + F(f(x_{i-1}), x_{i-1}) \right) + O(h^6), \quad (1.56)$$

$F(f(x), x)$ terms in the RHS are replaced by $-a(x) \cdot f(x)$. Then gathering $f(x_{i+1})$ in the RHS, we get eq. (1.55).

Sequence of points in actual calculations

In our program, sequence of points are separated by some blocks, and in each block points are equally separated. Table 1.1 describes the default sequence.

Table 1.1: Default sequence of points. FP and LP represent the first point and last point.

FP index	LP index	Distance	Number of distances	FP position	LP position
0	40	0.0025	40	0	0.1
40	80	0.005	40	0.1	0.3
80	120	0.01	40	0.3	0.7
120	160	0.02	40	0.7	1.5
160	200	0.04	40	1.5	3.1
200	240	0.08	40	3.1	6.3
240	280	0.16	40	6.3	12.7
280	320	0.32	40	12.7	25.5
320	360	0.64	40	25.5	51.1
360	400	1.28	40	51.1	102.3
400	440	2.56	40	102.3	204.7

1.2.2 Calculations of the Thomas-Fermi potential

The differential equation for the Thomas-Fermi potential is

$$\frac{d}{dx^2}g(x) = F(g(x), x) = \frac{g(x)^{3/2}}{\sqrt{x}}. \quad (1.57)$$

Since Numerov method is not applicable to the equation, we solve it by Euler method or 4th-order Runge-Kutta method. We note that only Euler method is applicable when we consider points belonging to different blocks, because the distance is not uniform.

The boundary condition derives the initial value $g(0) = 1$, but $g'(0)$ can not be determined. Therefore, we need to find appropriate $g'(0)$ satisfying the other boundary condition $g(x) \rightarrow 0$ ($x \rightarrow \infty$). In addition, if $g(x_i)$ becomes negative, we can not calculate $g(x_{i+1})$ and further because we cannot perform the three-halves power calculation.

In our actual calculations, we use the bisubsection method to find $g'(0)$ which gives $g(x_N)$ smaller than the threshold. Here we represent the value $g(x_N)$ calculated with the initial value $g'(0) = g'$ by $g(x_N; g')$; if $g(x_i) < 0$ occurs during calculations, we suppose $g(x_N; g') = g(x_i)$. The following is the detailed procedure of calculations.

1. Find g'_0 and g'_1 , which satisfy $g(x_N; g'_0) < 0 < g(x_N; g'_1)$.
2. Take $g'_2 = (g'_0 + g'_1)/2$ and calculate $g(x_N; g'_2)$.
3. If $g(x_N; g'_2) < 0$, replace g'_0 by g'_2 . If $g(x_N; g'_2) > 0$ and larger than the threshold, replace g'_1 by g'_2 . If $g(x_N; g'_2) > 0$ and smaller than the threshold, current $g(x_i)$ is the solution.

4. Unless $g(x_N; g'_2) > 0$ and smaller than the threshold, go back to 2. and continue calculations.

Figure 1.1 represents $g(x)$ obtained by our numerical calculations, which is approximately equal to the previous research [3].

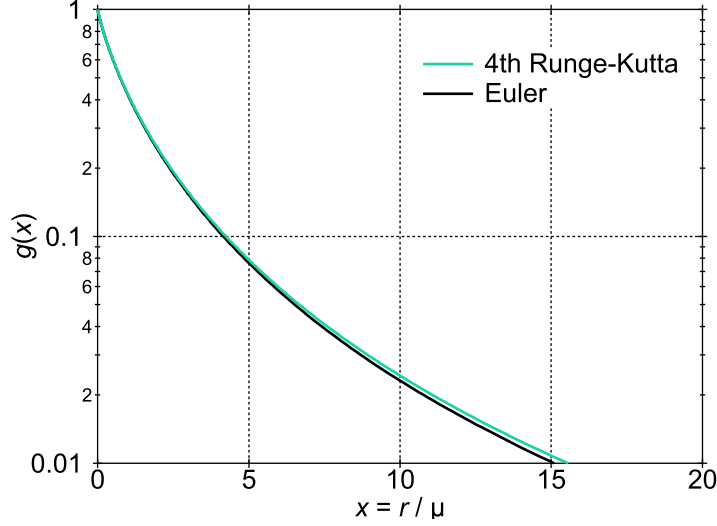


Figure 1.1: Thomas-Fermi potential function $g(x)$.

1.2.3 Schrödinger equation in an isotropic potential

Calculation procedure

The potential in the HFS equation $V(r)$ is isotropic, so we need to solve the Schrödinger equation of the radial part;

$$\left[-\frac{1}{2} \frac{d^2}{dr^2} + \frac{l(l+1)}{2r^2} + V(r) \right] P_{nl}(r) = E_{nl} P_{nl}(r). \quad (1.58)$$

Using the Thomas-Fermi scaling $r = \mu x$ and the substitution $P_{nl}(r) = p_{nl}(x)$, $V(r) = v(x)$, we get

$$\frac{d^2}{dx^2} p_{nl}(x) = \left[\frac{l(l+1)}{x^2} + 2\mu^2(v(x) - E_{nl}) \right] p_{nl}(x). \quad (1.59)$$

Since the potential values at points x_i , $v(x_i)$, are given, we can use Euler method or Numerov method. We cannot use 4th-order Runge-Kutta method because it uses the value at $x_i + h/2$. We find the solution with $n - l - 1$ nodes and eigenvalue E_{nl} . Bound solutions, which are regular at the origin, should satisfy $p_{nl}(0) = 0$ and $p_{nl}(x) \rightarrow 0$ ($x \rightarrow \infty$). The following condition is approximated to $p_{nl}(x_N) = 0$, where x_N is the last point of calculations.

We can use similar procedure to that of the Thomas-Fermi potential, to obtain $p_{nl}(x_i)$ with initial conditions at the origin $p_{nl}(0) = 0$; for $p'_{nl}(0)$ we can set an arbitrary value. However, this procedure gives large numerical error in large x region, so it is difficult to obtain E_{nl} satisfying $p_{nl}(x_N) = 0$ by the bisection method. Therefore, we use the following procedure to calculate $p_{nl}(x_i)$ with given E_{nl} .

1. The function in the RHS of eq. (1.59), $l(l+1)/x^2 + 2\mu^2(v(x) - E_{nl})$, becomes $-E_{nl} > 0$ in the limit $x \rightarrow \infty$. Therefore, if E_{nl} is an appropriate eigenvalue, $p_{nl}(x)$ increases/decreases monotonically and does not have a node in $x > x_0$ region, where x_0 is the last border across which the function changes sign (from negative to positive).
2. We set the calculation region to $0 \leq x < x_0 \times \text{const.}$ An appropriate const. is around 8, and if the last point is smaller than $x_0 \times \text{const.}$ the former is the calculation border.
3. We solve the differential equation from $x = 0$ to outward in $0 \leq x \leq x_0$ region and obtain $p_{nl}^{\text{out}}(x_i)$. On the other hand, in $x_0 \leq x$ region the equation is solved from the border to inward and we obtain $p_{nl}^{\text{in}}(x_i)$. In both calculations, the initial values of the differential are given arbitrarily.

4. We count the number of nodes only in $0 \leq x \leq x_0$ region.
5. Since eq. (1.59) is a linear differential equation, a solution multiplied by a constant is also a solution. We can scale $p_{nl}^{\text{out}}(x_i)$ and $p_{nl}^{\text{in}}(x_i)$ so that they are continuous at $x = x_0$. If the differentials are also continuous, the solution is appropriate. We can use the logarithmic derivative $\frac{1}{p_{nl}(x)} \frac{d}{dx} p_{nl}(x) = \frac{d}{dx} \log(p_{nl}(x))$ to judge the continuity of the differential.
6. If the logarithmic derivatives do not coincide, We can estimate the error ΔE by the method in the following subsubsection.

First we perform 1.-4. to obtain largest E_{nl} with $n-l-1$ nodes². After this estimation, we perform 1.-6. to change the estimated value of the eigenenergy. We continue this process until $|\Delta E|$ is smaller than the threshold, and then we obtain the eigenvalue E_{nl} , and the wavefunction is obtained by normalizing $p_{nl}(x_i)$.

Estimation of the eigenenergy error from logarithmic derivatives

Modifying eq. (1.59), we use the following differential equation

$$\frac{d^2}{dx^2} p(x) + (V(x) - \varepsilon) p(x) = 0 \quad (1.60)$$

and boundary conditions $p(0) = 0$, $p(x) \rightarrow 0$ ($x \rightarrow \infty$), where $p(x)$ is the solution and ε is the eigenenergy. Using a solution $q(x) = p(x) + \Delta p(x)$ and eigenenergy $\varepsilon + \Delta\varepsilon$, which satisfies the boundary conditions but is not continuous or differentiable at $x = x_0$, we estimate the eigenenergy error $\Delta\varepsilon$.

Since $q(x)$ and $\varepsilon + \Delta\varepsilon$ satisfy eq. (1.60) at any point other than $x = x_0$, inserting them and taking the first order of the error, we obtain

$$\frac{d^2}{dx^2} \Delta p(x) + (V(x) - \varepsilon) \Delta p(x) - \Delta\varepsilon \cdot p(x) = 0. \quad (1.61)$$

Multiplying $p(x)$ and performing integration, we get

$$\int_0^{x_0} \left[p(x) \frac{d^2}{dx^2} \Delta p(x) + (V(x) - \varepsilon) p(x) \Delta p(x) - \Delta\varepsilon \cdot p(x)^2 \right] dx = 0 \quad (1.62)$$

$$\iff \int_0^{x_0} \left[p(x) \frac{d^2}{dx^2} \Delta p(x) - \Delta p(x) \frac{d^2}{dx^2} p(x) \right] dx = \Delta\varepsilon \int_0^{x_0} p(x)^2 dx \quad (\because \text{Using eq. (1.60) to } (V(x) - \varepsilon)p(x)) \quad (1.63)$$

$$\iff \left[p(x) \frac{d}{dx} \Delta p(x) - \Delta p(x) \frac{d}{dx} p(x) \right]_0^{x_0} = \Delta\varepsilon \int_0^{x_0} p(x)^2 dx \quad (1.64)$$

$$\iff \left[p(x)^2 \Delta \left(\frac{1}{p(x)} \frac{d}{dx} p(x) \right) \right]_0^{x_0} = \Delta\varepsilon \int_0^{x_0} p(x)^2 dx \quad (1.65)$$

$$\iff p(x_0)^2 \Delta \left(\frac{1}{p(x_0)} \frac{d}{dx} p(x_0) \right) = \Delta\varepsilon \int_0^{x_0} p(x)^2 dx \quad (\because p(0) = 0). \quad (1.66)$$

We can obtain the similar result by changing the integration region to $[x_0, \infty]$. Modifying these results by using $q(x)$, we get

$$p(x_0)^2 \left[\frac{1}{q(x_0 - 0)} \frac{d}{dx} q(x_0 - 0) - \frac{1}{p(x_0)} \frac{d}{dx} p(x_0) \right] = \Delta\varepsilon \int_0^{x_0} p(x)^2 dx \quad (1.67)$$

$$-p(x_0)^2 \left[\frac{1}{q(x_0 + 0)} \frac{d}{dx} q(x_0 + 0) - \frac{1}{p(x_0)} \frac{d}{dx} p(x_0) \right] = \Delta\varepsilon \int_{x_0}^{\infty} p(x)^2 dx. \quad (1.68)$$

We replace $p(x)$ by $q(x)$ because we cannot obtain $p(x)$, and modifying the equations to remove the second term in the LHS, we get

$$\Delta\varepsilon = \frac{\frac{1}{q(x_0 - 0)} \frac{d}{dx} q(x_0 - 0) - \frac{1}{q(x_0 + 0)} \frac{d}{dx} q(x_0 + 0)}{\frac{1}{q(x_0 - 0)^2} \int_0^{x_0} q(x)^2 dx + \frac{1}{q(x_0 + 0)^2} \int_{x_0}^{\infty} q(x)^2 dx}. \quad (1.69)$$

²If the energy increases slightly from E_{nl} , where E_{nl} is a solution satisfying the boundary and node-number conditions, the node increases by 1.

As you can see from the equation, we can use $p_{nl}^{\text{out}}(x_i)$ and $p_{nl}^{\text{in}}(x_i)$ without the scaling to the error estimation.

Calculation examples using the Thomas-Fermi potential

Figure 1.2 shows the Z dependence of eigenenergies of the Schrödinger equation with the Thomas-Fermi potential. This result coincides well with the previous research [3].

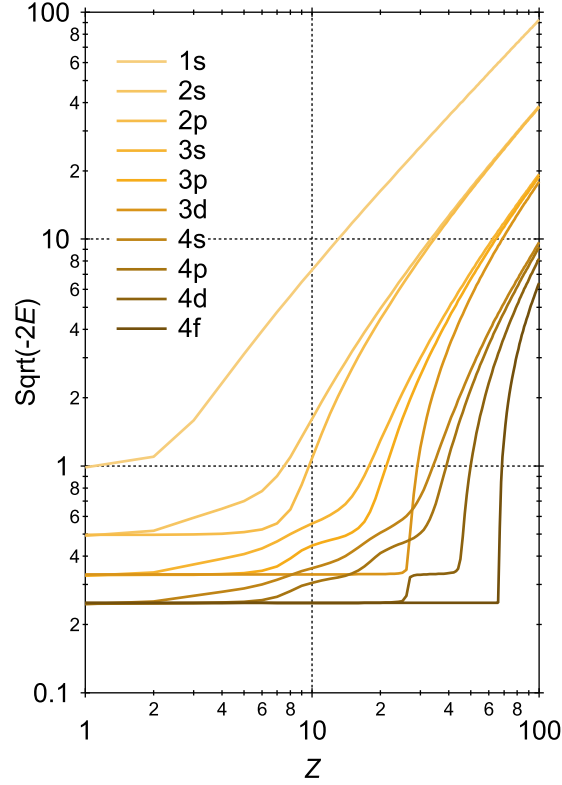


Figure 1.2: Eigenenergies in the Thomas-Fermi potential. Since the previous research [3] uses the Rydberg unit system, the vertical axis is $\sqrt{-2E}$, not $\sqrt{-E}$.

1.2.4 Calculations of self-consistent atomic potentials

Modification of the potential

As discussed above, the potential $V(r)$ in the HFS equation is given by

$$V(r) = -\frac{Z}{r} + \frac{1}{r} \int_0^r \sigma(r') dr' + \int_r^\infty \frac{\sigma(r')}{r'} dr' - 3 \left(\frac{3\rho(r)}{8\pi} \right)^{1/3} \quad (1.70)$$

$$\sigma(r) = \sum_{nl} w_{nl} (P_{nl}(r))^2 \quad (1.71)$$

$$\rho(r) = \frac{\sigma(r)}{4\pi r^2}. \quad (1.72)$$

In our actual calculations, we use the scaling $r = \mu x$, so the equations become

$$V(x_i) = -\frac{Z}{\mu x_i} + \frac{1}{x_i} \sum_{j=0}^{i-1} \sigma(x_j) (x_{j+1} - x_j) + \sum_{j=i}^{N-1} \frac{\sigma(x_j)}{x_j} (x_{j+1} - x_j) - 3 \left(\frac{3\rho(x_i)}{8\pi} \right)^{1/3} \quad (1.73)$$

$$\sigma(x_i) = \sum_{nl} w_{nl} (P_{nl}(x_i))^2 \quad (1.74)$$

$$\rho(x_i) = \frac{\sigma(x_i)}{4\pi (\mu x_i)^2}. \quad (1.75)$$

Furthermore, the potential should satisfy $V(x_i) \sim -1/\mu x_i$ in $x \rightarrow \infty$ limit, so we add the following modification:

$$V_{\text{modified}}(x_i) = \begin{cases} V(x_i) & V(x_i) < -\frac{1}{\mu x_i} \\ -\frac{1}{\mu x_i} & V(x_i) > -\frac{1}{\mu x_i} \end{cases}. \quad (1.76)$$

The radial Schrödinger equation (1.59) with the modified potential $V_{\text{modified}}(x_i)$ is solved.

SCF convergence

the j -th calculation is performed using the j -th input potential $V^{(j)}(x_i)$, $V_{\text{modified}}^{(j)}(x_i)$. After that, the potential for the $j+1$ -th calculation is obtained by the simple mixing method. We represent the potential obtained by the j -th calculation by $V(x_i)$, $V_{\text{modified}}(x_i)$, and then the $j+1$ -th input is

$$V^{(j+1)}(x_i) = (1-A)V(x_i) + A \cdot V^{(j)}(x_i), \quad V_{\text{modified}}^{(j+1)}(x_i) = (1-A)V_{\text{modified}}(x_i) + A \cdot V_{\text{modified}}^{(j)}(x_i) \quad (1.77)$$

. The mixing ratio A is between 0 and 1, and $A = 0.5$ gave the appropriate convergence.

The convergence is checked by the following parameters α , β .

$$\alpha_j = \max_i \left| \frac{V^{(j)}(x_i) - V^{(j+1)}(x_i)}{V^{(j)}(x_i)} \right| \quad (1.78)$$

$$\beta_j = \max_i \left| \mu x_i V^{(j)}(x_i) - \mu x_i V^{(j+1)}(x_i) \right| \quad (1.79)$$

We finished the calculations when the both values are below the thresholds.

Calculation example

In case of the carbon atom, $Z = 6$ and the occupancy is $w_{10} = 2$, $w_{20} = 2$, $w_{21} = 2$. Figure 1.3 shows the calculation result in good coincidence with the previous research [2].

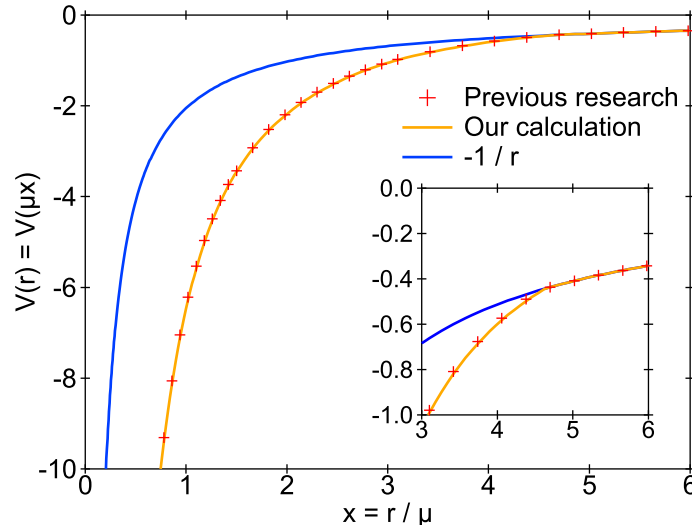


Figure 1.3: Self-consistent atomic potential of a carbon atom. The inset shows the border where the modification $V(x) = -1/\mu x$ starts.

1.3 Special functions for radial wave functions

We discuss the properties of special functions necessary for wave functions in a spherically isotropic potential $V(r)$.

1.3.1 Gamma functions

Definition

The gamma function is the natural extension of the factorial $n!$ defined by

$$\Gamma(x) = \int_0^\infty e^{-t} t^{x-1} dt. \quad (1.80)$$

Properties

When $x = 1$, we get

$$\Gamma(1) = \int_0^\infty e^{-t} dt = 1. \quad (1.81)$$

Partial integration gives

$$\Gamma(x) = \int_0^\infty e^{-t} t^{x-1} dt \quad (1.82)$$

$$= \left[-e^{-t} t^{x-1} \right]_0^\infty + (x-1) \int_0^\infty e^{-t} t^{x-2} dt = (x-1) \Gamma(x-1). \quad (1.83)$$

From Eqs. (1.81) and (1.83), we get

$$\Gamma(n) = (n-1)(n-2) \cdot 1 \cdot \Gamma(1) = (n-1)! \quad (1.84)$$

where n is a positive integer.

Next we consider the case where x is a half-integer. Since

$$\Gamma(1/2) = \int_0^\infty e^{-t} t^{-1/2} dt \quad (1.85)$$

$$= 2 \int_0^\infty e^{-u^2} du \quad (t = u^2, \quad dt = 2u du) \quad (1.86)$$

$$= \sqrt{\pi}, \quad (1.87)$$

we get

$$\Gamma(n+1/2) = (n-1/2)(n-3/2) \cdot 1/2 \cdot \Gamma(1/2) \quad (1.88)$$

$$= \frac{(2n-1)!}{(n-1)! \cdot 2^{n-1}} \sqrt{\pi} \quad (1.89)$$

$$= \frac{(2n-1)!}{(n-1)! \cdot 2^{2n-1}} \sqrt{\pi} \quad (n \geq 1). \quad (1.90)$$

Multiplying the denominator and numerator by $2n$, we get

$$\Gamma(n+1/2) = \frac{(2n)!}{n! \cdot 2^{2n}} \sqrt{\pi}, \quad (1.91)$$

which can be applicable for the $n = 0$ case.

Since Eq. (1.80) does not diverge unless x is zero or a negative integer, we can extend the gamma function to the complex space. For an arbitrary complex number z , the following relation holds;

$$\Gamma(z^*) = \int_0^\infty e^{-t} t^{z^*-1} dt = \left[\int_0^\infty e^{-t} t^{z-1} dt \right]^* = \Gamma(z)^*. \quad (1.92)$$

1.3.2 Bessel functions, spherical Bessel functions

The solutions of the Schrödinger equation with $V(r) = 0$ can be represented by a spherical Bessel function. Further transformation gives the relation between spherical Bessel functions and Bessel functions.

Transformation of a spherical Bessel function to a Bessel function

The Schrödinger equation with $V(r) = 0$ can be transformed to the spherical Bessel equation by the relation $x = kr$. The spherical Bessel equation is

$$\left[x^2 \frac{d^2}{dx^2} + 2x \frac{d}{dx} + (x^2 - l(l+1)) \right] j_l(x) = 0. \quad (1.93)$$

Then we consider the transformation of the spherical Bessel equation to the following Bessel equation.

$$\left[x^2 \frac{d^2}{dx^2} + x \frac{d}{dx} + (x^2 - \nu^2) \right] J_\nu(x) = 0. \quad (1.94)$$

From the relation $j_l(x) = x^{-1/2} f(x)$, we get

$$\frac{d}{dx} j_l(x) = x^{-1/2} \frac{df(x)}{dx} - \frac{1}{2} x^{-3/2} f(x) \quad (1.95)$$

$$\frac{d^2}{dx^2} j_l(x) = x^{-1/2} \frac{d^2 f(x)}{dx^2} - x^{-3/2} \frac{df(x)}{dx} + \frac{3}{4} x^{-5/2} f(x). \quad (1.96)$$

Substituting the above equations, we get

$$\left[x^2 \frac{d^2}{dx^2} + x \frac{d}{dx} + (x^2 - (l+1/2)^2) \right] f(x) = 0. \quad (1.97)$$

The result gives the relation between a spherical Bessel function $j_l(x)$ and a Bessel function $J_\nu(x)$;

$$j_l(x) = \sqrt{\frac{\pi}{2x}} J_{l+1/2}(x). \quad (1.98)$$

The coefficient $\sqrt{\pi/2}$ is multiplied for a convenience later.

Series expansion of a Bessel function

We obtain a Bessel function $J_\nu(x)$ by series expansion. Hereafter, some of arguments are based on the assumption that ν is a half integer $l + 1/2$.

First, the Bessel function is expanded like

$$J_\nu(x) = \sum_{j=0}^{\infty} a_j x^{c+j}, \quad a_0 \neq 0. \quad (1.99)$$

Derivatives of the above equation is

$$\frac{d}{dx} J_\nu(x) = \sum_{j=0}^{\infty} a_j (c+j) x^{c+j-1} \quad (1.100)$$

$$\frac{d^2}{dx^2} J_\nu(x) = \sum_{j=0}^{\infty} a_j (c+j)(c+j-1) x^{c+j-2}. \quad (1.101)$$

Substituting them, we get

$$\sum_{j=0}^{\infty} a_j \left[((c+j)^2 - \nu^2) x^{c+j} + x^{c+j+2} \right] = 0. \quad (1.102)$$

Looking at only the x^{c+j} terms, we get

$$j = 0, 1: a_j((c+j)^2 - \nu^2) = 0 \quad (1.103)$$

$$j \geq 2: a_j((c+j)^2 - \nu^2) + a_{j-2} = 0 \iff a_j = \frac{-1}{(c+j)^2 - \nu^2} a_{j-2} \text{ (when } (c+j)^2 - \nu^2 \neq 0). \quad (1.104)$$

From the condition $a_0 \neq 0$, $c = \pm\nu$ is derived.

Next we consider the equation for the $j = 1$ case. The term in the parentheses becomes $(c+j)^2 - \nu^2 = \pm 2\nu + 1$, so $a_1 = 0$ is necessary for the cases other than $\nu = \pm 1/2$. Therefore, all terms with odd j vanish from Eq. (1.104). The following argument proves that the assumption $a_1 = 0$ does not lose generality even in the $\nu = \pm 1/2$ case. When $\nu = 1/2$, the solution with $c = -\nu = -1/2$ can have nonzero a_1 while $c = \nu = 1/2$ cannot. Here we introduce $X(x, y) = -1/(x^2 - y^2)$, corresponding $x = c + j$, $y = \nu$. Then the solutions are

$$c = \nu = 1/2: J_\nu(x) = a_0 x^{1/2} + X(5/2, 1/2) a_0 x^{5/2} + X(9/2, 1/2) X(5/2, 1/2) a_0 x^{9/2} + \dots \quad (1.105)$$

$$c = -\nu = -1/2: J_\nu(x) = a_0 x^{-1/2} + X(3/2, 1/2) a_0 x^{3/2} + X(7/2, 1/2) X(3/2, 1/2) a_0 x^{7/2} \dots \\ + a_1 x^{1/2} + X(5/2, 1/2) a_1 x^{5/2} + X(9/2, 1/2) X(5/2, 1/2) a_1 x^{9/2} + \dots \quad (1.106)$$

However, the terms with a_1 in Eq. (1.106) is the same as Eq. (1.105) \times (a constant) so they can be removed. Therefore we can assume $a_1 = 0$. The $\nu = -1/2$ case is also discussed similarly.

From the arguments, a_j can be nonzero when $j = 2k$ ($k = 0, 1, \dots$). Since ν is a half-integer, the demoninator in Eq. (1.104) cannot be nonzero because $j = \mp 2\nu$ is not satisfied³ Therefore, a_{2k} can be obtained inductively from a_0 .

First, when $c = \nu$ we get

$$X(c+j, \nu) = -\frac{1}{(\nu+j)^2 - \nu^2} = \frac{-1}{j(2\nu+j)}. \quad (1.107)$$

The recursion equation (1.104) gives

$$a_{2k} = \frac{-1}{4k(\nu+k)} a_{2k-2} \quad (1.108)$$

$$= \frac{-1}{4k(k+j)} \frac{-1}{4(k-1)(\nu+k-1)} a_{2k-4} \quad (1.109)$$

$$= \dots = \frac{(-1)^k}{2^{2k} k! \cdot (\nu+k) \dots (\nu+1)} a_0. \quad (1.110)$$

Since Eq. (1.83) gives

$$(\nu+k) \dots (\nu+1) = \frac{\Gamma(\nu+k+1)}{\Gamma(\nu+1)}, \quad (1.111)$$

we get

$$a_{2k} = \frac{(-1)^k \Gamma(\nu+1)}{2^{2k} k! \cdot \Gamma(\nu+k+1)} a_0, \quad (1.112)$$

and supposing

$$a_0 = \frac{1}{2^\nu \Gamma(\nu+1)} \quad (1.113)$$

we finally obtain

$$a_{2k} = \frac{(-1)^k}{2^{2k+\nu} k! \cdot \Gamma(\nu+k+1)} \quad (1.114)$$

³if ν is an integer and $c = -\nu$, Eq. (1.104) with the $j = 2\nu$ case gives $a_{2\nu-2} = 0$. Going back the recursion equation, we get $a_0, \dots, a_{2\nu-2} = 0$. Therefore the first nonzero term is $a_{2\nu}$. In this case, the solution is equivalent to the $c = \nu$ case.

となる。

When $c = -\nu$, we get

$$X(c + j, \nu) = \frac{-1}{j(-2\nu + j)} \quad (1.115)$$

$$a_{2k} = \frac{(-1)^k}{2^{2k-\nu} k! \cdot \Gamma(-\nu + k + 1)} \quad (a_0 = 1/(2^{-\nu} \Gamma(-\nu + 1))). \quad (1.116)$$

In summary, two solutions of the Bessel equation are

$$J_\nu(x) = \left(\frac{x}{2}\right)^\nu \sum_{k=0}^{\infty} \frac{(-1)^k}{k! \cdot \Gamma(\nu + k + 1)} \left(\frac{x}{2}\right)^{2k} \quad (1.117)$$

and $J_{-\nu}(x)$.

Neumann functions

When ν is not an integer, $J_\nu(x)$ and $J_{-\nu}(x)$ are linearly independent solutions of the Bessel equation. The Neumann function defined by

$$Y_\nu(x) = \frac{1}{\sin(\nu\pi)} (\cos(\nu\pi) J_\nu(x) - J_{-\nu}(x)) \quad (1.118)$$

is frequently used instead of $J_{-\nu}(x)$. However, when $\nu = l + 1/2$ the difference between $Y_{l+1/2}(x)$ and $J_{-(l+1/2)}(x)$ is only the sign since

$$Y_{l+1/2}(x) = (-1)^{l+1} J_{-(l+1/2)}(x) \quad (1.119)$$

$y_l(x) = \sqrt{\pi/2x} \cdot Y_{l+1/2}(x)$ is called as the spherical Neumann function, which diverges at $x = 0$.

Recursion formula of Bessel functions

$J_\nu(x)$ satisfies the following recursion formula;

$$\frac{d}{dx} (x^{-\nu} J_\nu(x)) = -x^{-\nu} J_{\nu+1}(x). \quad (1.120)$$

The series expansion gives the proof as follows;

$$\frac{d}{dx} (x^{-\nu} J_\nu(x)) = \sum_{k=0}^{\infty} \frac{(-1)^k}{k! \cdot \Gamma(\nu + k + 1)} \frac{2kx^{2k-1}}{2^{2k+\nu}} \quad (1.121)$$

$$= \sum_{k=1}^{\infty} \frac{(-1)^k}{(k-1)! \cdot \Gamma(\nu + k + 1)} \frac{x^{2k-1}}{2^{2k+\nu-1}} \quad (k=0 \text{ term is zero}) \quad (1.122)$$

$$= \sum_{K=0}^{\infty} \frac{-(-1)^K}{K! \cdot \Gamma(\nu + K + 2)} \frac{x^{2K+1}}{2^{2K+\nu+1}} \quad (K = k-1) \quad (1.123)$$

$$= -x^{-\nu} \sum_{K=0}^{\infty} \frac{(-1)^K}{K! \cdot \Gamma(\nu + K + 2)} \left(\frac{x}{2}\right)^{2K+\nu+1} \quad (1.124)$$

$$= -x^{-\nu} J_{\nu+1}(x). \quad (1.125)$$

The Bessel functions also satisfy the following formula;

$$\frac{d}{dx} (x^\nu J_\nu(x)) = x^\nu J_{\nu-1}(x). \quad (1.126)$$

The series expansion gives

$$\frac{d}{dx} \left(x^\nu J_\nu(x) \right) = \sum_{k=0}^{\infty} \frac{(-1)^k}{k! \cdot \Gamma(\nu + k + 1)} \frac{(2k + 2\nu)x^{2k+2\nu-1}}{2^{2k+\nu}} \quad (1.127)$$

$$= \sum_{k=1}^{\infty} \frac{(-1)^k}{(k-1)! \cdot \Gamma(\nu + k)} \frac{x^{2k+2\nu-1}}{2^{2k+\nu-1}} \quad (\because \Gamma(\nu + k + 1) = (\nu + k)\Gamma(\nu + k)) \quad (1.128)$$

$$= x^\nu \sum_{k=0}^{\infty} \frac{(-1)^k}{k! \cdot \Gamma(\nu + k)} \left(\frac{x}{2} \right)^{2k+\nu-1} \quad (1.129)$$

$$= x^\nu J_{\nu-1}(x). \quad (1.130)$$

Spherical Bessel functions and spherical Neumann functions

The recursion formula above and the Bessel function with $\nu = 1/2$,

$$J_{1/2}(x) = \sqrt{\frac{x}{2}} \sum_{k=0}^{\infty} \frac{(-1)^k}{k! \cdot \Gamma(k + 1 + 1/2)} \left(\frac{x}{2} \right)^{2k} \quad (1.131)$$

$$= \sqrt{\frac{x}{2}} \sum_{k=0}^{\infty} \frac{(-1)^k (k+1)! \cdot 2^{2k+2}}{k! \cdot (2k+2)! \cdot \sqrt{\pi}} \left(\frac{x}{2} \right)^{2k} \quad (\because (1.91)) \quad (1.132)$$

$$= \sqrt{\frac{2}{\pi x}} \sum_{k=0}^{\infty} \frac{(-1)^k}{(2k+1)!} x^{2k+1} = \sqrt{\frac{2}{\pi x}} \sin x, \quad (1.133)$$

the Bessel function when ν is a positive half-integer becomes

$$J_{l+1/2}(x) = -x^{l-1/2} \frac{d}{dx} \left(x^{-(l-1/2)} J_{l-1/2}(x) \right) \quad (1.134)$$

$$= -x^{l-1/2} \frac{d}{dx} \left(-\frac{1}{x} \frac{d}{dx} \left(x^{-(l-3/2)} J_{l-3/2}(x) \right) \right) \quad (1.135)$$

$$= (-1)^l x^{l+1/2} \left(\frac{1}{x} \frac{d}{dx} \right)^l x^{-1/2} J_{1/2}(x) \quad (1.136)$$

$$= \sqrt{\frac{2}{\pi}} (-1)^l x^{l+1/2} \left(\frac{1}{x} \frac{d}{dx} \right)^l \frac{\sin x}{x}. \quad (1.137)$$

The spherical Bessel function is represented by

$$j_l(x) = (-1)^l x^l \left(\frac{1}{x} \frac{d}{dx} \right)^l \frac{\sin x}{x}. \quad (1.138)$$

The following are spherical Bessel functions from $l = 0$ to $l = 4$.

$$j_0(x) = \frac{\sin x}{x} \quad (1.139)$$

$$j_1(x) = \frac{\sin x - x \cos x}{x^2} \quad (1.140)$$

$$j_2(x) = \frac{(3 - x^2) \sin x - 3x \cos x}{x^3} \quad (1.141)$$

$$j_3(x) = \frac{(15 - 6x^2) \sin x + (x^3 - 15x) \cos x}{x^4} \quad (1.142)$$

$$j_4(x) = \frac{(x^4 - 45x^2 + 105) \sin x + (10x^3 - 105x) \cos x}{x^5} \quad (1.143)$$

The Bessel function with $\nu = -1/2$ is

$$J_{-1/2}(x) = \sqrt{\frac{2}{x}} \sum_{k=0}^{\infty} \frac{(-1)^k}{k! \cdot \Gamma(k + 1/2)} \left(\frac{x}{2}\right)^{2k} \quad (1.144)$$

$$= \sqrt{\frac{2}{x}} \sum_{k=0}^{\infty} \frac{(-1)^k k! \cdot 2^{2k}}{k! \cdot (2k)! \cdot \sqrt{\pi}} \left(\frac{x}{2}\right)^{2k} \quad (\because (1.91)) \quad (1.145)$$

$$= \sqrt{\frac{2}{\pi x}} \sum_{k=0}^{\infty} \frac{(-1)^k}{(2k)!} x^{2k} = \sqrt{\frac{2}{\pi x}} \cos x. \quad (1.146)$$

Therefore, the Bessel function when ν is a negative half-integer is

$$J_{-l-1/2}(x) = x^{l-1/2} \frac{d}{dx} \left(x^{-l+1/2} J_{-l+1/2}(x) \right) \quad (1.147)$$

$$= x^{l-1/2} \frac{d}{dx} \left(\frac{1}{x} \frac{d}{dx} \left(x^{-l+3/2} J_{-l+3/2}(x) \right) \right) \quad (1.148)$$

$$= x^{l+1/2} \left(\frac{1}{x} \frac{d}{dx} \right)^l x^{-1/2} J_{-1/2}(x) \quad (1.149)$$

$$= \sqrt{\frac{2}{\pi}} x^{l+1/2} \left(\frac{1}{x} \frac{d}{dx} \right)^l \frac{\cos x}{x}. \quad (1.150)$$

The spherical Neumann function is

$$y_l(x) = (-1)^{l+1} x^l \left(\frac{1}{x} \frac{d}{dx} \right)^l \frac{\cos x}{x}. \quad (1.151)$$

Asymptotic forms

The asymptotic forms with $x \rightarrow 0$ is dominated by the lowest power of x in the series expansion. Therefore, we get

$$J_\nu(x) \sim \left(\frac{x}{2}\right)^\nu \frac{1}{\Gamma(\nu + 1)} \quad (1.152)$$

and

$$j_l(x) \sim \sqrt{\frac{\pi}{2x}} \left(\frac{x}{2}\right)^{l+1/2} \frac{1}{\Gamma(l + 1 + 1/2)} \quad (1.153)$$

$$= \sqrt{\frac{\pi}{2x}} \left(\frac{x}{2}\right)^{l+1/2} \frac{(l+1)! \cdot 2^{2l+2}}{(2l+2)! \cdot \sqrt{\pi}} \quad (\because (1.91)) \quad (1.154)$$

$$= \frac{2^l l!}{(2l+1)!} x^l. \quad (1.155)$$

The asymptotic forms with $x \rightarrow \infty$ is dominated by the term obtained by the differentiations of the trigonometric function. Therefore, the form of the spherical Bessel function is

$$j_l(x) \sim (-1)^l \frac{1}{x} \frac{d^l}{dx^l} \sin x \quad (1.156)$$

$$= \frac{1}{x} \frac{(-1)^l}{2i} \left(i^l \cis(x) - (-i)^l \cis(-x) \right) \quad (1.157)$$

$$= \frac{1}{x} \frac{\cis(x - l\pi/2) - \cis(-(x - l\pi/2))}{2i} \quad (1.158)$$

$$= \frac{\sin(x - l\pi/2)}{x} \quad (1.159)$$

and that of the spherical Neumann function is

$$y_l(x) \sim (-1)^{l+1} \frac{1}{x} \frac{d^l}{dx^l} \cos x \quad (1.160)$$

$$= \frac{1}{x} \frac{(-1)^{l+1}}{2} \left(i^l \text{cis}(x) + (-i)^l \text{cis}(-x) \right) \quad (1.161)$$

$$= \frac{-1}{x} \frac{\text{cis}(x - l\pi/2) + \text{cis}(-(x - l\pi/2))}{2} \quad (1.162)$$

$$= -\frac{\cos(x - l\pi/2)}{x}, \quad (1.163)$$

where $\text{cis}(x) = e^{ix} = \cos x + i \sin x$.

1.3.3 Coulomb wave functions

A Coulomb function is a solution of the Schrödinger equation with the Coulomb potential $V(r) = -1/r$.

Transformation to a confluent hypergeometric function

Substituting $E = k^2/2$ and $r = x/k$ in the radial Schrödinger equation with the Coulomb potential, we get

$$\left[\frac{d^2}{dx^2} + 1 + \frac{2}{kx} - \frac{l(l+1)}{x^2} \right] f(x) = 0. \quad (1.164)$$

First, the equation is transformed to the Whittaker equation

$$\left[\frac{d^2}{dz^2} - \frac{1}{4} + \frac{\kappa}{z} + \frac{1/4 - \mu^2}{z^2} \right] g(z) = 0. \quad (1.165)$$

Using the relation $x = z/2i$, we get

$$(1.164) \iff \left[-4 \frac{d^2}{dz^2} + 1 + \frac{4i}{kz} + \frac{4l(l+1)}{z^2} \right] f(z/2i) = 0 \quad (1.166)$$

$$\iff \left[\frac{d^2}{dz^2} - \frac{1}{4} - \frac{i}{kz} + \frac{1/4 - (l+1/2)^2}{z^2} \right] f(z/2i) = 0. \quad (1.167)$$

Therefore we get the following relation;

$$g(z) = f(x) = f(z/2i), \quad \kappa = -\frac{i}{k}, \quad \mu = l + \frac{1}{2}. \quad (1.168)$$

Next, the Whittaker equation is transformed to the confluent hypergeometric equation

$$\left[z \frac{d^2}{dz^2} + (b-z) \frac{d}{dz} - a \right] h(z) = 0. \quad (1.169)$$

Assuming the relation $g(z) = e^{-z/2} z^{\mu+1/2} h(z)$, the derivatives of it are

$$\frac{d}{dz} g(z) = -\frac{1}{2} e^{-z/2} z^{\mu+1/2} h(z) + (\mu + 1/2) e^{-z/2} z^{\mu-1/2} h(z) + e^{-z/2} z^{\mu+1/2} \frac{dh(z)}{dz} \quad (1.170)$$

$$\begin{aligned} \frac{d^2}{dz^2} g(z) &= \frac{1}{4} e^{-z/2} z^{\mu+1/2} h(z) + (\mu^2 - 1/4) e^{-z/2} z^{\mu-3/2} h(z) + e^{-z/2} z^{\mu+1/2} \frac{d^2 h(z)}{dz^2} \\ &\quad + 2 \left[-\frac{\mu + 1/2}{2} e^{-z/2} z^{\mu-1/2} h(z) - \frac{1}{2} e^{-z/2} z^{\mu+1/2} \frac{dh(z)}{dz} + (\mu + 1/2) e^{-z/2} z^{\mu-1/2} \frac{dh(z)}{dz} \right]. \end{aligned} \quad (1.171)$$

Therefore, we get

$$(1.165) \iff \left[\frac{d^2}{dz^2} + \left(-1 + \frac{2\mu+1}{z} \right) \frac{d}{dz} + \frac{\kappa - (\mu+1/2)}{z} \right] h(z) = 0 \quad (1.172)$$

$$\iff \left[z \frac{d^2}{dz^2} + (2\mu + 1 - z) \frac{d}{dz} - (\mu - \kappa + 1/2) \right] h(z) = 0. \quad (1.173)$$

The relation between the Whittaker equation and the confluent hypergeometric equation becomes

$$b = 2\mu + 1 = 2(l + 1), \quad a = \mu - \kappa + \frac{1}{2} = l + 1 + \frac{i}{k}. \quad (1.174)$$

Regular and irregular solutions of the confluent hypergeometric function are represented by $M(a, b, z)$ and $U(a, b, z)$, respectively. $M(a, b, z)$ is

$$M(a, b, z) = \sum_{s=0}^{\infty} \frac{(a)_s}{(b)_s s!} z^s, \quad (1.175)$$

where $(a)_s$ is the Pochhammer symbol defined by

$$(a)_s = a(a+1) \cdots (a+s-1), \quad (a)_0 = 1. \quad (1.176)$$

$U(a, b, z)$ has different representations depending on a and b . In this case, $U(a, b, z)$ is

$$\begin{aligned} U(a, n+1, z) &= \frac{(-1)^{n+1}}{n! \Gamma(a-n)} \sum_{k=0}^{\infty} \frac{(a)_k}{(n+1)_k k!} z^k (\log z + \psi(a+k) - \psi(1+k) - \psi(n+k+1)) \\ &\quad + \frac{1}{\Gamma(a)} \sum_{k=1}^n \frac{(k-1)!(1-a+k)_{n-k}}{(n-k)!} z^{-k}, \quad n = 0, 1, \dots, a \neq 0, -1, \dots \end{aligned} \quad (1.177)$$

$$\psi(x) = \frac{1}{\Gamma(x)} \frac{d\Gamma(x)}{dx}. \quad (1.178)$$

$\psi(x)$ is called as the digamma function.

Normalization based on the asymptotic forms

The asymptotic forms of $M(a, b, z)$ and $U(a, b, z)$ with $z \rightarrow \infty$ are

$$\begin{aligned} M(a, b, z) &\sim \frac{\Gamma(b)}{\Gamma(a)} e^z z^{a-b} \sum_{s=0}^{\infty} \frac{(1-a)_s (b-a)_s}{s!} z^{-s} \\ &\quad + \frac{\Gamma(b)}{\Gamma(b-a)} e^{i\pi a} z^{-a} \sum_{s=0}^{\infty} \frac{(a)_s (a-b+1)_s}{s!} (-z)^{-s}, \quad -\frac{\pi}{2} + \delta \leq \arg z \leq \frac{3\pi}{2} - \delta \end{aligned} \quad (1.179)$$

$$U(a, b, z) \sim z^{-a} \sum_{s=0}^{\infty} \frac{(a)_s (a-b+1)_s}{s!} (-z)^{-s}, \quad |\arg z| \leq \frac{3\pi}{2} - \delta. \quad (1.180)$$

Since $z = 2ix$ and $x \geq 0$, the argument of z becomes $\frac{\pi}{2}$

We extract the highest power of x in the asymptotic forms. For $M(a, b, z)$, the highest power from the first term is z^{a-b} , that from the second term is z^{-a} , and

$$z^{a-b} = (2ix)^{-(l+1)+i/k} \quad (1.181)$$

$$= (2x)^{-(l+1)+i/k} \times \exp\left(\frac{\pi i}{2} \cdot (-(l+1) + i/k)\right) \quad (1.182)$$

$$= (2x)^{-(l+1)} e^{-\pi/2k} \text{cis} \left[\frac{\log(2x)}{k} - \frac{\pi(l+1)}{2} \right] \quad (1.183)$$

$$z^{-a} = (2ix)^{-(l+1)-i/k} \quad (1.184)$$

$$= (2x)^{-(l+1)-i/k} \times \exp\left(\frac{\pi i}{2} \cdot (-(l+1) - i/k)\right) \quad (1.185)$$

$$= (2x)^{-(l+1)} e^{\pi/2k} \text{cis} \left[-\frac{\log(2x)}{k} - \frac{\pi(l+1)}{2} \right]. \quad (1.186)$$

Since these are the same order, both of them are taken into account, and multiplying the conversion coefficient $e^{-z/2}z^{\mu+1/2}$ we get

$$e^{-ix}(2ix)^{l+1} \left[\frac{\Gamma(2(l+1))}{\Gamma(l+1+i/k)} e^{2ix}(2x)^{-(l+1)} e^{-\pi/2k} \text{cis} \left(\frac{\log(2x)}{k} - \frac{\pi(l+1)}{2} \right) + \frac{\Gamma(2(l+1))}{\Gamma(l+1-i/k)} e^{i\pi(l+1+i/k)} (2x)^{-(l+1)} e^{\pi/2k} \text{cis} \left(-\frac{\log(2x)}{k} - \frac{\pi(l+1)}{2} \right) \right] \quad (1.187)$$

$$= i^{l+1}(2l+1)! e^{-\pi/2k} \left[\frac{e^{ix}}{\Gamma(l+1+i/k)} \text{cis} \left(\frac{\log(2x)}{k} - \frac{\pi(l+1)}{2} \right) + \frac{e^{-ix}}{\Gamma(l+1-i/k)} \text{cis} \left(-\frac{\log(2x)}{k} + \frac{\pi(l+1)}{2} \right) \right] \quad (1.188)$$

$$= \frac{(-i)i^{l+1}(2l+1)!e^{-\pi/2k}}{|\Gamma(l+1+i/k)|} \left[\text{cis} \left(x + \frac{\log(2x)}{k} - \frac{l\pi}{2} + \arg \Gamma(l+1-i/k) \right) - \text{c.c.} \right] \quad (1.189)$$

$$= \frac{2 \cdot i^{l+1}(2l+1)!e^{-\pi/2k}}{|\Gamma(l+1+i/k)|} \sin \left(x + \frac{\log(2x)}{k} - \frac{l\pi}{2} + \arg \Gamma(l+1-i/k) \right). \quad (1.190)$$

Eq. (1.92) is used during the transformation and c.c. represents the complex conjugate of the first term. $f(x)$ is normalized as follows

$$f_1(x) = \frac{|\Gamma(l+1+i/k)| \cdot e^{\pi/2k}}{2k \cdot (2l+1)!} e^{-ix}(2x)^{l+1} M(l+1+i/k, 2l+2, 2ix) \quad (1.191)$$

$$f_1(kr) \rightarrow \frac{1}{k} \sin \left(kr + \frac{\log(2kr)}{k} - \frac{l\pi}{2} + \arg \Gamma(l+1-i/k) \right), \quad (1.192)$$

so that the asymptotic form of $f(kr)/r$ becomes similar to that of the spherical Bessel function $j_l(kr) \rightarrow \sin(kr - l\pi/2)/kr$.

For $U(a, b, z)$, the asymptotic form of the highest power is z^{-a} so

$$e^{-ix}(2ix)^{l+1}(2ix)^{-(l+1)-i/k} = e^{\pi/2k} \text{cis}(-x - \log(2x)/k) \quad (1.193)$$

is the asymptotic form of the Coulomb wave function. A linear combination of it and $f(x)$ gives the solution with the following asymptotic form

$$f_2(kr) \rightarrow \frac{1}{k} \cos \left(kr + \frac{\log(2kr)}{k} - \frac{l\pi}{2} + \arg \Gamma(l+1-i/k) \right). \quad (1.194)$$

At last, we discuss the behavior of $f_1(x)$ around $x \rightarrow 0$. Since $M(a, b, z) \rightarrow 1$, we get

$$f_1(x) \rightarrow \frac{|\Gamma(l+1+i/k)| \cdot e^{\pi/2k}}{2k \cdot (2l+1)!} (2x)^{l+1}. \quad (1.195)$$

Therefore, we need to set the sign of $f_1(x)$ so that the first derivative is positive.

Real function

We prove that

$$f_0(x) = e^{-ix}(2x)^{l+1} M(l+1-i/k, 2l+2, -2ix), \quad (1.196)$$

obtained by removing real coefficients in $f_1(x)$, is a real function

From Eq. (1.175), we get

$$M(a, b, z)^* = M(a^*, b^*, z^*). \quad (1.197)$$

Also using the relation derived from the confluent hypergeometric equation

$$M(a, b, z) = e^z M(b-a, b, -x), \quad (1.198)$$

We get

$$f_0^*(x) = e^{ix}(2x)^{l+1} M(l+1-i/k, 2l+2, -2ix) \quad (1.199)$$

$$= e^{ix}(2x)^{l+1} e^{-2ix} M(l+1+i/k, 2l+2, 2ix) \quad (1.200)$$

$$= e^{-ix}(2x)^{l+1} M(l+1+i/k, 2l+2, 2ix) = f_0(x). \quad (1.201)$$

Therefore $f_0(x)$ is a real function.

1.3.4 Spherical harmonics

A spherical harmonic is an eigenstate of the angular momentum operator.

Conversion of polar coordinate system and cartesian coordinate system

The position vector \mathbf{r} is represented by polar and cartesian coordinates like

$$\mathbf{r} = \begin{pmatrix} x \\ y \\ z \end{pmatrix} = \begin{pmatrix} r \sin \theta \cos \varphi \\ r \sin \theta \sin \varphi \\ r \cos \theta \end{pmatrix}. \quad (1.202)$$

The partial derivative of a function with respect to the distance r gives

$$f(r + \Delta r, \theta, \varphi) - f(r, \theta, \varphi) = \Delta r \frac{\partial}{\partial r} f(\mathbf{r}). \quad (1.203)$$

When we represent the relation using the cartesian coordinates, we get

$$f(r + \Delta r, \theta, \varphi) - f(r, \theta, \varphi) = f(x + \Delta r \sin \theta \cos \varphi, y + \Delta r \sin \theta \sin \varphi, z + \Delta r \cos \theta) - f(x, y, z) \quad (1.204)$$

$$= \Delta r \left[\sin \theta \cos \varphi \frac{\partial}{\partial x} + \sin \theta \sin \varphi \frac{\partial}{\partial y} + \cos \theta \frac{\partial}{\partial z} \right] f(\mathbf{r}). \quad (1.205)$$

Comparing them, we get

$$\frac{\partial}{\partial r} = \sin \theta \cos \varphi \frac{\partial}{\partial x} + \sin \theta \sin \varphi \frac{\partial}{\partial y} + \cos \theta \frac{\partial}{\partial z}. \quad (1.206)$$

Similar arguments give

$$\frac{\partial}{\partial \theta} = r \cos \theta \cos \varphi \frac{\partial}{\partial x} + r \cos \theta \sin \varphi \frac{\partial}{\partial y} - r \sin \theta \frac{\partial}{\partial z} \quad (1.207)$$

$$\frac{\partial}{\partial \varphi} = -r \sin \theta \sin \varphi \frac{\partial}{\partial x} + r \sin \theta \cos \varphi \frac{\partial}{\partial y}, \quad (1.208)$$

and the inverse transformations are

$$\frac{\partial}{\partial x} = \sin \theta \cos \varphi \frac{\partial}{\partial r} + \frac{\cos \theta \cos \varphi}{r} \frac{\partial}{\partial \theta} - \frac{\sin \varphi}{r \sin \theta} \frac{\partial}{\partial \varphi} \quad (1.209)$$

$$\frac{\partial}{\partial y} = \sin \theta \sin \varphi \frac{\partial}{\partial r} + \frac{\cos \theta \sin \varphi}{r} \frac{\partial}{\partial \theta} + \frac{\cos \varphi}{r \sin \theta} \frac{\partial}{\partial \varphi} \quad (1.210)$$

$$\frac{\partial}{\partial z} = \cos \theta \frac{\partial}{\partial r} - \frac{\sin \theta}{r} \frac{\partial}{\partial \theta}. \quad (1.211)$$

Using these relations, the following relations can be proved;

$$\Delta = \frac{1}{r^2} \frac{\partial}{\partial r} r^2 \frac{\partial}{\partial r} - \frac{\mathbf{L}^2}{r^2}, \quad \mathbf{L} = \mathbf{r} \times \mathbf{p} = -i\mathbf{r} \times \nabla \quad (1.212)$$

$$L_z = -i \left(x \frac{\partial}{\partial y} - y \frac{\partial}{\partial x} \right) = -i \frac{\partial}{\partial \varphi} \quad (1.213)$$

$$L_{\pm} = L_x \pm iL_y = e^{\pm i\varphi} \left(\pm \frac{\partial}{\partial \theta} + i \frac{\cos \theta}{\sin \theta} \frac{\partial}{\partial \varphi} \right). \quad (1.214)$$

Derivation of spherical harmonics

We obtain the eigenstate of \mathbf{L}^2 and L_z satisfying

$$\mathbf{L}^2 Y_{lm}(\theta, \varphi) = l(l+1) Y_{lm}(\theta, \varphi) \quad (1.215)$$

$$L_z Y_{lm}(\theta, \varphi) = m Y_{lm}(\theta, \varphi). \quad (1.216)$$

First, from Eqs. (1.213) and (1.216) the spherical harmonic can be decomposed like

$$Y_{lm}(\theta, \varphi) = \Theta(\theta)\Phi(\varphi) \quad (1.217)$$

$$L_z\Phi(\varphi) = -i\frac{\partial}{\partial\varphi}\Phi(\varphi) = m\Phi(\varphi). \quad (1.218)$$

The normalization is defined so that the integrals with respect to θ and φ become 1;

$$\int_0^\pi \sin\theta d\theta \int_0^{2\pi} d\varphi |Y_{lm}(\theta, \varphi)|^2 = \int_0^\pi |\Theta(\theta)|^2 \sin\theta d\theta \int_0^{2\pi} |\Phi(\varphi)|^2 d\varphi = 1 \times 1. \quad (1.219)$$

The differential equation with respect to φ can be easily solved; the solution is

$$\Phi_m(\varphi) = \frac{1}{\sqrt{2\pi}} e^{im\varphi}. \quad (1.220)$$

The coefficient $1/\sqrt{2\pi}$ is for the normalization.

Next we obtain $\Theta(\theta)$. From the properties of the ladder operator L_\pm , when $m = l$ we get

$$L_+(\Theta_l(\theta)\Phi_l(\varphi)) = 0 \quad (1.221)$$

$$\iff \left[\frac{\partial}{\partial\theta} - l \frac{\cos\theta}{\sin\theta} \right] \Theta_l(\theta) = 0. \quad (1.222)$$

The solution of the above equation is

$$\Theta_l(\theta) = (-1)^l \sqrt{\frac{(2l+1)!}{2}} \frac{1}{2^l l!} \sin^l \theta. \quad (1.223)$$

The normalization of the solution is determined from

$$I_l = \frac{2l}{2l+1} \frac{2l-2}{2l-1} \cdots \frac{2}{3} I_0 = \frac{2 \cdot (2^l l!)^2}{(2l+1)!}, \quad (1.224)$$

which is obtained from

$$I_l = \int_0^\pi \sin^{2l+1} \theta d\theta = 2l \int_0^\pi (1 - \sin^2 \theta) \sin^{2l-1} \theta d\theta = 2l(I_{l-1} - I_l) \quad (1.225)$$

$$\therefore I_l = \frac{2l}{2l+1} I_{l-1} \quad (1.226)$$

and $I_0 = 2$. The coefficient $(-1)^l$ is multiplied for a convenience later.

Since we get $\Theta_l(\theta)$, we can calculate Θ_{lm} from the properties of the latter operator

$$L_- Y_{lm}(\theta, \varphi) = \sqrt{(l+m)(l-m+1)} Y_{lm-1}(\theta, \varphi). \quad (1.227)$$

Since

$$L_- \Theta_{lm}(\theta) \Phi_m(\varphi) = \left(-\frac{\partial}{\partial\theta} - m \frac{\cos\theta}{\sin\theta} \right) \Theta_{lm}(\theta) \Phi_{m-1}(\varphi) \quad (1.228)$$

holds, we get

$$\Theta_{lm-1}(\theta) = -\frac{1}{\sqrt{(l+m)(l-m+1)}} \left(\frac{d}{d\theta} + m \frac{\cos\theta}{\sin\theta} \right) \Theta_{lm}(\theta). \quad (1.229)$$

Here we introduce the conversion $x = \cos\theta$. Since $dx = -\sin\theta d\theta$,

$$\sin^{1-m} \theta \frac{d}{dx} [\sin^m \theta \cdot f(\theta)] = \sin\theta \frac{d}{dx} f(\theta) - m \cos\theta \frac{d\theta}{dx} f(\theta) = -\left(\frac{d}{d\theta} + m \frac{\cos\theta}{\sin\theta} \right) f(\theta) \quad (1.230)$$

holds. Substituting it, we get

$$\Theta_{lm-1}(\theta) = \frac{\sin^{1-m} \theta}{\sqrt{(l+m)(l-m+1)}} \frac{d}{dx} [\sin^m \theta \cdot \Theta_{lm}(\theta)]. \quad (1.231)$$

Using it repeatedly, finally we get

$$\Theta_{lm}(\theta) = \sqrt{\frac{(l+m)!}{(2l)!(l-m)!}} \frac{1}{\sin^m \theta} \left(\frac{d}{dx} \right)^{l-m} \sin^l \theta \cdot \Theta_{ll}(\theta) \quad (1.232)$$

$$= (-1)^l \sqrt{\frac{2l+1}{2}} \frac{(l+m)!}{(l-m)!} \frac{1}{2^l l!} \frac{1}{\sin^m \theta} \left(\frac{d}{dx} \right)^{l-m} \sin^{2l} \theta. \quad (1.233)$$

Similar argument gives

$$\Theta_{lm+1}(\theta) = -\frac{\sin^{1+m} \theta}{\sqrt{(l-m)(l+m+1)}} \frac{d}{dx} \left[\sin^{-m} \theta \cdot \Theta_{lm}(\theta) \right]. \quad (1.234)$$

Especially when $m = 0$, the spherical harmonic becomes

$$\Theta_{l0}(\theta) = (-1)^l \sqrt{\frac{2l+1}{2}} \frac{1}{2^l l!} \left(\frac{d}{dx} \right)^l \sin^{2l} \theta = \sqrt{\frac{2l+1}{2}} P_l(\cos \theta), \quad (1.235)$$

where

$$P_l(x) = \frac{1}{2^l l!} \left(\frac{d}{dx} \right)^l (x^2 - 1)^l \quad (1.236)$$

is the Legendre polynomial derived by the Roudrigues formula. Here we obtain Θ_{lm} from Θ_{l0} ; the result is

$$\Theta_{lm}(\theta) = (-1)^m \sqrt{\frac{2l+1}{2} \frac{(l-m)!}{(l+m)!}} \sin^m \theta \left(\frac{d}{dx} \right)^m P_l(x) \quad (1.237)$$

$$\Theta_{l-m}(\theta) = \sqrt{\frac{2l+1}{2} \frac{(l-m)!}{(l+m)!}} \sin^m \theta \left(\frac{d}{dx} \right)^m P_l(x) = (-1)^m \Theta_{lm}(\theta), \quad (1.238)$$

where m is limited so that $m \geq 0$.

Explicit formulae

First, the Legendre polynomials are

$$P_0(x) = 1 \quad (1.239)$$

$$P_1(x) = x \quad (1.240)$$

$$P_2(x) = \frac{3}{2}x^2 - \frac{1}{2} \quad (1.241)$$

$$P_3(x) = \frac{5}{2}x^3 - \frac{3}{2}x \quad (1.242)$$

$$P_4(x) = \frac{35}{8}x^4 - \frac{15}{4}x^2 + \frac{3}{8}. \quad (1.243)$$

Applying the ladder operators on $\Theta_{ll}(\theta)$, we can obtain the explicit formulae of $\Theta_{lm}(\theta)$. In the following $\Theta_{l-m}(\theta)$ are omitted because the relation $(-1)^m \Theta_{lm}(\theta)$ gives $\Theta_{l-m}(\theta)$.

$$\Theta_{00}(\theta) = \frac{1}{\sqrt{2}} \quad (1.244)$$

$$\Theta_{11}(\theta) = -\frac{\sqrt{3}}{2} \sin \theta \quad (1.245)$$

$$\Theta_{10}(\theta) = \sqrt{\frac{3}{2}} \cos \theta \quad (1.246)$$

$$\Theta_{22}(\theta) = \frac{\sqrt{15}}{4} \sin^2 \theta \quad (1.247)$$

$$\Theta_{21}(\theta) = -\frac{\sqrt{15}}{2} \sin \theta \cos \theta \quad (1.248)$$

$$\Theta_{20}(\theta) = \frac{1}{2} \sqrt{\frac{5}{2}} (3 \cos^2 \theta - 1) \quad (1.249)$$

$$\Theta_{33}(\theta) = -\frac{\sqrt{70}}{8} \sin^3 \theta \quad (1.250)$$

$$\Theta_{32}(\theta) = \frac{\sqrt{105}}{4} \sin^2 \theta \cos \theta \quad (1.251)$$

$$\Theta_{31}(\theta) = -\frac{\sqrt{42}}{8} (5 \cos^2 \theta - 1) \sin \theta \quad (1.252)$$

$$\Theta_{30}(\theta) = \frac{1}{2} \sqrt{\frac{7}{2}} (5 \cos^2 \theta - 3) \cos \theta \quad (1.253)$$

$$\Theta_{44}(\theta) = \frac{3\sqrt{35}}{16} \sin^4 \theta \quad (1.254)$$

$$\Theta_{43}(\theta) = -\frac{3\sqrt{70}}{8} \sin^3 \theta \cos \theta \quad (1.255)$$

$$\Theta_{42}(\theta) = \frac{3\sqrt{5}}{8} (7 \cos^2 \theta - 1) \sin^2 \theta \quad (1.256)$$

$$\Theta_{41}(\theta) = -\frac{3\sqrt{10}}{8} (7 \cos^2 \theta - 3) \sin \theta \cos \theta \quad (1.257)$$

$$\Theta_{40}(\theta) = \frac{3\sqrt{2}}{16} (35 \cos^4 \theta - 20 \cos^2 \theta + 3) \quad (1.258)$$

1.3.5 Partial wave expansion

The plane wave $e^{i\mathbf{k}\cdot\mathbf{r}}$ can be expanded by spherical Bessel functions and spherical harmonics.

When \mathbf{k} is parallel to the z axis, the partial wave expansion is

$$e^{ikr \cos \theta} = \sum_l i^l (2l+1) j_l(kr) P_l(\cos \theta). \quad (1.259)$$

The proof is as follows.

The plane wave $e^{ikr \cos \theta}$ is a solution of the Schrödinger equation without potential ($E = k^2/2$). On the other hand, $j_l(kr) Y_{lm}(\theta, \varphi)$ are also solutions with the same eigenenergy and they form a complete set. Therefore the plane wave should be represented by a linear combination of them. The φ -independent property shows that we only need to consider the $m = 0$ case, we assume

$$e^{ikr \cos \theta} = \sum_l c_l j_l(kr) P_l(\cos \theta). \quad (1.260)$$

The asymptotic form of the spherical Bessel function with $r \rightarrow 0$ is given by Eq. (1.155), which shows that $j_l(kr)$ is the l -th power of r . The l -th power terms in $P_l(x)$ is obtained from Eq. (1.236) like

$$\frac{1}{2^l l!} \left(\frac{d}{dx} \right)^l x^{2l} = \frac{(2l)!}{2^l (l!)^2} x^l. \quad (1.261)$$

Comparing the $(kr \cos \theta)^l$ terms of the left hand side and the right hand side, finally we obtain

$$\frac{1}{l!} (ikr \cos \theta)^l = c_l \frac{2^l l! (kr)^l (2l)! \cdot \cos^l \theta}{(2l+1)! 2^l (l!)^2} = \frac{c_l}{(2l+1)l!} (kr \cos \theta)^l \quad \therefore c_l = i^l (2l+1). \quad (1.262)$$

Next we consider an arbitrary \mathbf{k} . We represent the directions of \mathbf{r} and \mathbf{k} by (θ, φ) and (θ_k, φ_k) , and the angle between \mathbf{r} and \mathbf{k} by ω . Then we get

$$e^{i\mathbf{k}\cdot\mathbf{r}} = e^{ikr \cos \omega} = \sum_l i^l (2l+1) j_l(kr) P_l(\cos \omega). \quad (1.263)$$

Using the addition theorem of spherical harmonics

$$P_l(\cos \omega) = \frac{4\pi}{2l+1} \sum_m Y_{lm}^*(\theta_k, \varphi_k) Y_{lm}(\theta, \varphi), \quad (1.264)$$

finally we obtain

$$e^{i\mathbf{k}\cdot\mathbf{r}} = 4\pi \sum_{lm} i^l j_l(kr) Y_{lm}^*(\theta_k, \varphi_k) Y_{lm}(\theta, \varphi). \quad (1.265)$$

1.4 Photoemission angular distribution calculations

We explain the method to calculate the matrix element of the photoemission based on the one-electron approximation and dipole approximation.

1.4.1 Overview

In the photoemission process, the perturbation Hamiltonian due to the light irradiation $\delta H(t)$ is

$$\delta H(t) = \frac{1}{2}(\hat{\mathbf{p}} \cdot \mathbf{A}(t) + \mathbf{A}(t) \cdot \hat{\mathbf{p}}) \quad (1.266)$$

$$= \frac{A_0}{2}(\hat{\mathbf{p}} \cdot \mathbf{e}e^{i\mathbf{k}^L \cdot \mathbf{r}} + \mathbf{e}e^{i\mathbf{k}^L \cdot \mathbf{r}} \cdot \hat{\mathbf{p}})e^{-i\omega t} \quad (1.267)$$

$$= \delta H e^{-i\omega t}, \quad (1.268)$$

where $\hat{\mathbf{p}}$ is the momentum operator, $\mathbf{A}(t)$ the vector potential of the light, \mathbf{e} a unit vector representing the polarization, \mathbf{k}^L the wavevector of the light, and ω is the angular frequency of the light. We represent the time-independent part of the perturbation by δH as used in Eq. (1.268). According to Fermi's golden rule, the excitation probability by the perturbation is

$$p(|\psi^I\rangle \rightarrow |\psi^F\rangle) = 2\pi\delta(E^F - E^I - \omega) \left| \langle \psi^F | \delta H | \psi^I \rangle \right|^2, \quad (1.269)$$

where $|\psi^I\rangle$ and E^I are the wave function and the eigenenergy for the initial state, $|\psi^F\rangle$ and E^F are those for the final state, and the delta function represents the energy conservation law. Therefore, we need to obtain initial and final states and a perturbation term due to the light electric field to calculate the matrix element in the excitation probability equation.

1.4.2 Initial states

An initial state is a Bloch state with a wavevector \mathbf{k} and a band index μ , and is represented by a linear combination of pseudo-atomic orbitals (LCAO) in OpenMX;

$$\psi_{\mu}^{(\mathbf{k})}(\mathbf{r}) = \frac{1}{\sqrt{N}} \sum_n e^{i\mathbf{R}_n \cdot \mathbf{k}} \sum_{i\alpha\sigma} c_{\mu,i\alpha}^{\sigma(\mathbf{k})} \phi_{i\alpha}(\mathbf{r} - \boldsymbol{\tau}_i - \mathbf{R}_n) |\sigma\rangle. \quad (1.270)$$

In the equation above, \mathbf{R}_n is a lattice vector, i an atom position index, $\alpha = (plm)$ an organized orbital index with the multiplicity index p , angular quantum number l , and magnetic quantum number m , σ (\uparrow or \downarrow) a spin index, $\phi(\mathbf{r})$ a pseudo-atomic orbital, and $\boldsymbol{\tau}_i$ an atom position vector. In this paper, the Bloch wavevector \mathbf{k} is in the extended zone scheme. We distinguish an imaginary unit i and an index i by capital and italic letters, respectively. $c_{\mu,i\alpha}^{\sigma(\mathbf{k})}$ is an LCAO coefficient of the wave function and can be directly obtained from OpenMX. See Sec. 2.1 for the details of the pseudo-atomic orbitals.

1.4.3 Final States

A final state, the wavefunction of a photoelectron, is roughly a plane wave, but it should be modified inside a solid crystal. First, the eigenenergy of the final state with the wavevector \mathbf{k} becomes $\frac{1}{2}|\mathbf{k}|^2 - V_0$, where V_0 is the inner potential of the material [18]. The dispersion of final states should be considered when we determine possible \mathbf{k} values where the photoemission occurs based on the energy conservation law. Second, atomic potentials can change the eigenstate from a simple plane wave to a plane wave plus an ingoing spherical wave [23]. The modification details are discussed after the derivation of the matrix element equation. At last, the wave functions of final states can rapidly decay into the bulk when we consider the surface sensitivity of ARPES measurements [20].

1.4.4 Perturbation term

As we discussed, the perturbation term due to the electric field is like Eq. 1.267. Since the initial state is a linear combination of localized PAOs or AOs, we can approximate $e^{i\mathbf{k}^L \cdot \mathbf{r}}$ by $e^{i\mathbf{k}^L \cdot (\boldsymbol{\tau}_i + \mathbf{R}_n)}$, where $\boldsymbol{\tau}_i + \mathbf{R}_n$

is the position of the i th atom. This constant is neglected because \mathbf{k}^L is much smaller than \mathbf{k} . By this dipole approximation and the relation $\hat{\mathbf{p}} = \frac{d}{dt}\hat{\mathbf{r}}$, we get

$$p(|\psi^I\rangle \rightarrow |\psi^F\rangle) = 2\pi\delta(E^F - E^I - \omega)(A_0\omega)^2 \left| \langle \psi^F | \mathbf{r} \cdot \mathbf{e} | \psi^I \rangle \right|^2. \quad (1.271)$$

Whatever the light polarization is, the $\mathbf{r} \cdot \mathbf{e}$ term can be represented by the linear combination of $rY_{1j}(\theta, \varphi)$ like $\mathbf{r} \cdot \mathbf{e} = \sum_{j=-1}^1 e_j rY_{1j}(\theta, \varphi)$, where e_j are coefficients depending on the light polarization and direction.

At this point, we introduce atomic potentials on final states to calculate the matrix element. When we calculate it for an orbital centered at $\boldsymbol{\tau}_i + \mathbf{R}_n$, we set the origin of the polar coordinate system at $\boldsymbol{\tau}_i + \mathbf{R}_n$, for an easier understanding of equations. The wave function of the orbital specified by $\alpha = (plm)$ is

$$\phi_{\alpha in}^{(\mathbf{k})I}(\mathbf{r}) = e^{i\mathbf{k} \cdot \mathbf{R}_n} Y_{lm}(\theta, \varphi) \frac{P_{ipl}^I(r)}{r}. \quad (1.272)$$

The plane wave, a final state neglecting the atomic potential, is

$$\psi_{in}^{(\mathbf{k})F}(\mathbf{r}) = 4\pi e^{i\mathbf{k} \cdot (\boldsymbol{\tau}_i + \mathbf{R}_n)} \sum_{l'm'} i^{l'} Y_{l'm'}^*(\hat{\mathbf{k}}) Y_{l'm'}(\theta, \varphi) j_{l'}(kr). \quad (1.273)$$

In the equation, the partial wave expansion is applied, $\hat{\mathbf{k}}$ represents the angles θ and φ of the vector \mathbf{k} , $j_l(x)$ is the spherical Bessel function, and k is equal to $|\mathbf{k}|$. When the potential $V_{at}(r)$ is taken into account, the modified final state becomes the sum of the plane wave and an ingoing spherical wave like

$$\psi_{in}^{(\mathbf{k})F}(\mathbf{r}) = 4\pi e^{i\mathbf{k} \cdot (\boldsymbol{\tau}_i + \mathbf{R}_n)} \sum_{l'm'} i^{l'} e^{-\delta_{il'}} Y_{l'm'}^*(\hat{\mathbf{k}}) Y_{l'm'}(\theta, \varphi) \frac{P_{il'}^F(r)}{r}. \quad (1.274)$$

Derivation of the above form is as follows. We can assume that $V_{at}(r)$ is very localized around $r = 0$ due to the screening effect of valence electrons. Therefore, we define r_0 so that $V_{at}(r) = 0$ if $r > r_0$ and the radial wave function outside of r_0 should have the following asymptotic form;

$$P_{il'}^F(r) \rightarrow \frac{1}{k} \sin(kr - l\pi/2 + \delta_{il'}). \quad (1.275)$$

The asymptotic form without $\delta_{il'}$ is identical to that of $rj_{l'}(kr)$, the solution without $V_{at}(r)$. The Schrödinger equation with $V_{at}(r)$ gives $P_{il'}^F(r)$, and the $e^{-\delta_{il'}}$ term is multiplied to remove outgoing spherical waves.

The integration of the initial state, the final state, and the perturbation term can be separated into the spherical harmonics part and the radial part. The spherical harmonics part is the integration of $Y_{l'm'}^* Y_{1j} Y_{lm}$, and the integral becomes nonzero when $l' = l \pm 1$ and $m' = m + j$ are satisfied [21].

$$\int Y_{l+1,m}^* Y_{1,0} Y_{lm} \sin \theta d\theta d\varphi = \sqrt{\frac{3}{4\pi}} \sqrt{\frac{(l+1)^2 - m^2}{(2l+3)(2l+1)}} \quad (1.276)$$

$$\int Y_{l-1,m}^* Y_{1,0} Y_{lm} \sin \theta d\theta d\varphi = \sqrt{\frac{3}{4\pi}} \sqrt{\frac{l^2 - m^2}{(2l-1)(2l+1)}} \quad (1.277)$$

$$\int Y_{l+1,m+1}^* Y_{1,1} Y_{lm} \sin \theta d\theta d\varphi = \sqrt{\frac{3}{4\pi}} \sqrt{\frac{(l+m+2)(l+m+1)}{2(2l+3)(2l+1)}} \quad (1.278)$$

$$\int Y_{l-1,m+1}^* Y_{1,1} Y_{lm} \sin \theta d\theta d\varphi = -\sqrt{\frac{3}{4\pi}} \sqrt{\frac{(l-m)(l-m-1)}{2(2l-1)(2l+1)}} \quad (1.279)$$

$$\int Y_{l+1,m-1}^* Y_{1,-1} Y_{lm} \sin \theta d\theta d\varphi = \sqrt{\frac{3}{4\pi}} \sqrt{\frac{(l-m+2)(l-m+1)}{2(2l+3)(2l+1)}} \quad (1.280)$$

$$\int Y_{l-1,m-1}^* Y_{1,-1} Y_{lm} \sin \theta d\theta d\varphi = -\sqrt{\frac{3}{4\pi}} \sqrt{\frac{(l+m)(l+m-1)}{2(2l-1)(2l+1)}} \quad (1.281)$$

This integral is related to the Gaunt coefficient [6], and we denote it as $g(l', m + j; l, m)$. The radial part is numerically calculated.

Summing up the integral over $\boldsymbol{\tau}_i$, \mathbf{R}_n , and α , we finally obtain

$$\langle \psi_{\sigma}^{(\mathbf{k})F} | \mathbf{r} \cdot \mathbf{e} | \psi_{\mu}^{(\mathbf{k})I} \rangle = 4\pi\sqrt{N} \sum_{i\alpha} \sum_{l'}^{l\pm 1} \sum_{j=-1}^1 (-i)^{l'} Y_{l',m+j}(\hat{\mathbf{k}}) e^{i(\delta_{il'} - \mathbf{k} \cdot \boldsymbol{\tau}_i)} e_j c_{\mu,i\alpha}^{\sigma(\mathbf{k})} g(l', m+j; l, m) \int_0^{\infty} r P_{il'}^F(r) P_{ipl}^I(r) dr. \quad (1.282)$$

Neglecting the $4\pi\sqrt{N}$ term in the beginning, we use the norm of the matrix element to draw the PAD. Since the final states are spin-degenerated, we can calculate the matrix element for each spin separately.

Since it is difficult to calculate the screened potential in solids, we instead use wave functions of excited states in an atom as discussed in Sec. 1.2. Since the potential becomes $-1/r$ at large r , the asymptotic form is slightly changed to

$$P_{il}(r) \rightarrow \frac{1}{k} \sin(kr - l\pi/2 + \log(2kr)/k + \delta_{il}). \quad (1.283)$$

The asymptotic form is similar to that of the Coulomb wave function (see Sec. 1.3.3 for the details).

Chapter 2

Software

2.1 Atomic and pseudo-atomic orbitals in OpenMX and ADPACK

OpenMX[9] is a first-principles calculation software package using localized basis sets and the pseudopotentials (PPs) for OpenMX are generated by ADPACK[10]. We explain the method to obtain the relationship between atomic orbitals (AOs) in the all-electron (AE) potential and pseudo-atomic orbitals (PAOs) in the PP. See Ref. [11] for properties of PPs.

2.1.1 Modification of ADPACK

ADPACK can perform AE calculations, PP calculations, and PAO calculations depending on the value of `calc.type` (ALL, VPS, and PAO respectively). We modified ADPACK as described in Table 2.1 to calculate AOs and PAOs up to unoccupied states. The modified package is available from this repository.

Table 2.1: Modification of ADPACK.

File name	Line number	Modifications
<code>adpack.h</code>	24-25	Constants <code>ASIZE11</code> , <code>ASIZE12</code> are enlarged.
<code>adpack.h</code>	38	<code>max_N</code> , the largest principal quantum number in AO calculations, is added.
<code>adpack.h</code>	185	The function <code>All_Electron_NSCF</code> is added.
<code>readfile.c</code>	123	It reads <code>max_N</code> from the keyword <code>max.N</code> .
<code>adpack.c</code>	145-146	It calculates of unoccupied states in AE calculations.
<code>All_Electron.c</code>	42-48, 655-659	It exchanges the flag value so that the AE calculations (<code>Calc.Type=0</code>) become identical to those for PAO calculations (<code>Calc.Type=2</code>).
<code>All_Electron_NSCF.c</code>	All	<code>All_Electron.c</code> is copied to <code>All_Electron_NSCF.c</code> , and then modified to calculate unoccupied AOs using the methods in Sec. 1.2.3.
<code>Output.c</code>	743-781	It outputs the AOs in <code>Output_AllBases</code> by the same format as the PAOs (ll. 927-944 in <code>Output_PAOBases2</code>)
<code>makefile</code>	29	<code>All_Electron_NSCF.o</code> is added in <code>OBJs</code> .

2.1.2 Comparison of orbitals

Here we use `C6.0.pao` as PAOs and `C_CA19.vps` as a PP. While they are used as inputs for OpenMX, parameters in the beginning can be used as the input for ADPACK. We performed AO and PAO calculations based on these input data, although they were slightly modified.

We note that the core potential for a carbon atom includes only the $1s$ orbital. Therefore, p and d orbitals have no change due to the pseudization.

AOs and PAOs (PP input)

We calculated AOs (wave functions in the AE potential) and PAOs (those in the PP) based on the input parameters in the PP file `C_CA19.vps`. Figure 2.1 shows the result for the $2s$ orbital. Since the $1s$ is included in the PP, the $2s$ orbital is the lowest eigenstate with no node.

Optimization of PAOs (PAO input)

Calculated PAOs are for an atom, so they are slightly different in solids or molecules. OpenMX optimizes PAOs by linear combinations in order to represent bonded states in solids and molecules by less number of bases [12]. The optimization can be checked by comparing PAOs (after the optimization) in the PAO file `C6.0.pao` and those recalculated from input parameters in the file (before the optimization) (Fig. 2.2). The linear combination coefficients are included in PAO files [13] and same values can be calculated by the inner product of the optimized PAOs and recalculated PAOs.

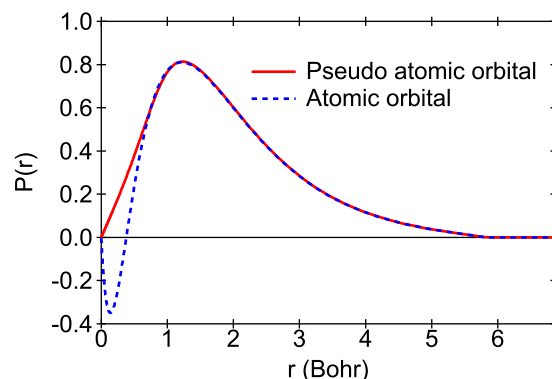


Figure 2.1: 2s AO and PAO for a carbon atom using the PP file as the input.

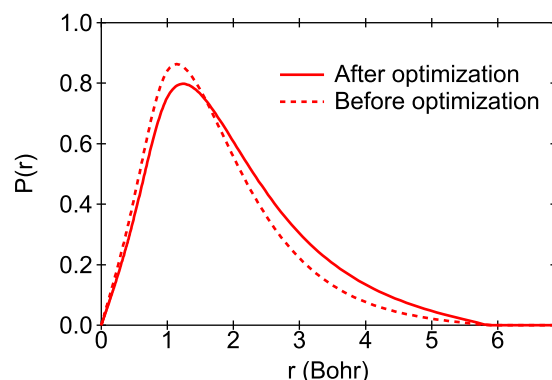


Figure 2.2: 2s PAOs before and after the optimization using the PAO file as the input.

We need to be careful of that the atom for PAO calculations may be different from that for PP calculations. In case of a carbon atom, AE calculations for PAOs use the 1s orbital occupied by 1.5 electrons (not 2.0), therefore the 2s orbitals are slightly different (Fig. 2.3).

Optimized PAOs, and corresponding AOs

Above arguments show that PAOs used in OpenMX are optimized and they are represented by linear combinations of original PAOs, eigenstates with the PP. AE calculations during PP calculations give correspondence PAOs (before optimization) and AOs. Therefore, AOs corresponding to optimized PAOs can be obtained by linear combination with the same coefficients as PAOs. Figure 2.4 shows the result for the carbon 2s orbital. The vertical line in the figure shows the cutoff of PP calculations (1.3 Bohr) and we can confirm that the PAO and AO are identical out of the cutoff.

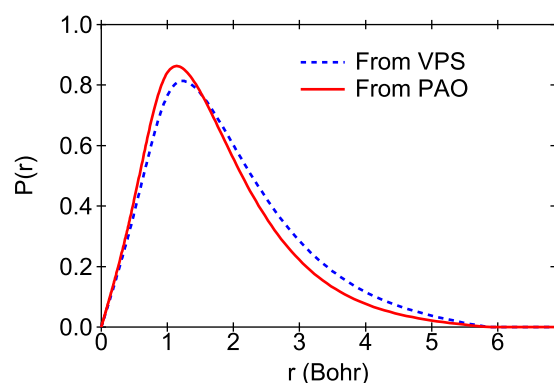


Figure 2.3: 2s PAOs using the PP and PAO files as the inputs.

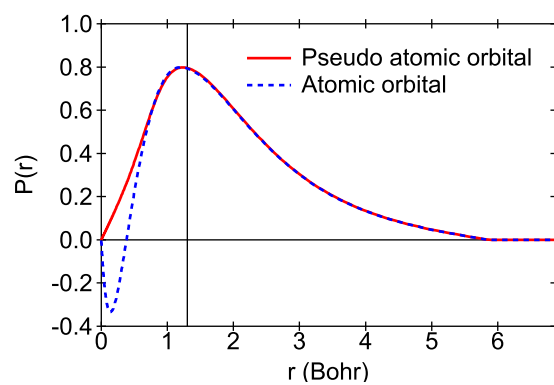


Figure 2.4: Optimized 2s PAO for a carbon atom and corresponding AO.

2.2 GUI_tools directory

Tools included in the `GUI_tools` directory are described. While they are unnecessary for actual photoemission calculations, they are useful for the visualization of data.

2.2.1 Overview

The following tools uses Python 3.7 and libraries listed in Table 2.2.

Table 2.2: Python libraries necessary for the tools. The versions are those for the development environment.

Library	Version
PyQt5	5.15.2
pyqtgraph	0.12.3
h5py	3.2.0
numpy	1.20.1
scipy	1.7.1

Each directory contains the template file `Config.example.py`. Users need to copy it to `Config.py` to execute the programs. Since `Config.py` is out of the Git control, they can modified it by themselves.

2.2.2 OpenMX_viewer

Data blocks beginning by *<keyword* and ending by *>keyword* frequently appears in OpenMX files. The tool can read it and draw a graph.

Figure 2.5 shows a pseudo-atomic orbital in C6.0.pao. In case of a function of the distance r like pseudo-atomic orbitals, the first column is $x = \log(r)$, the second column is r , and the other columns are values of the function [14].

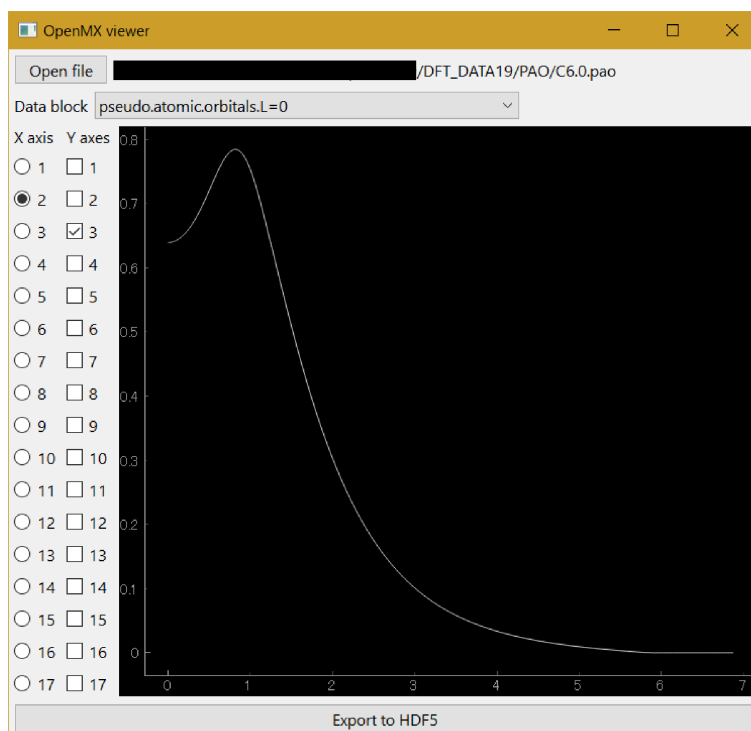


Figure 2.5: Example of `OpenMX_viewer.py`.

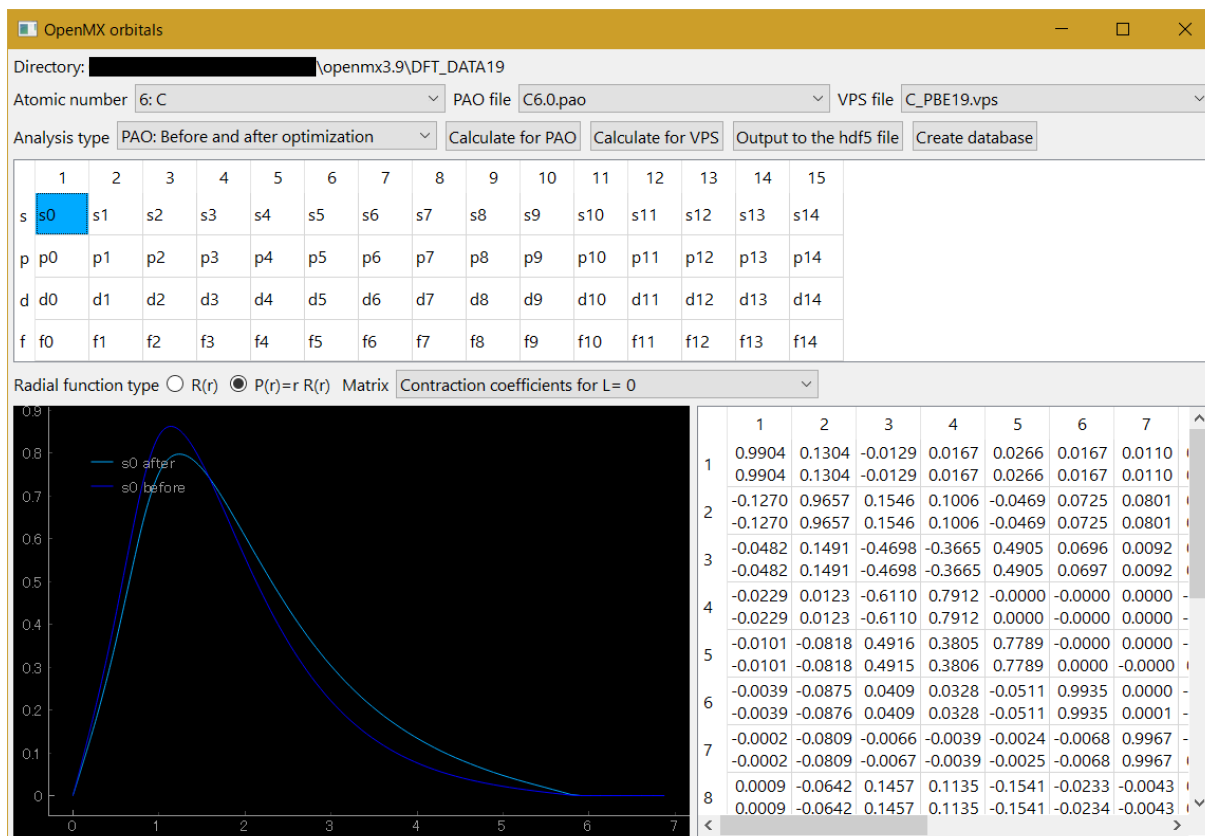


Figure 2.6: Example of `OpenMX_orbitals.py` showing pseudo-atomic orbitals before and after the optimization.

2.2.3 OpenMX_orbitals

The tool calculates AOs corresponding to optimized PAOs according to the method in Sec. 2.1. Since pseudopotential and pseudo-atomic orbital files in OpenMX include input parameters for ADPACK, these parameters are used for the following calculations.

1. Pseudo-atomic orbital calculations using the pseudopotential file
2. Atomic orbital calculations using the pseudopotential file
3. Pseudo-atomic orbital (before optimization) calculations using the pseud-atomic potential file

Users need to set `workingDirectory` (the directory containing pseudopotentials and pseudo-atomic orbitals of OpenMX) and `adpack` (the modified ADPACK executable) in `Config.py` before the execution. Since ADPACK needs a C compiler, `OpenMX_orbitals.py` also needs to be executed on the same environment. Once ADPACK completes calculations the other calculations are performed by Python. If you copy the data from ADPACK, you can continue calculations on different environments.

Figure 2.6 shows an example using `C6.0.pao` and `C_PBE19.vps`. Calculations are specified by `Analysis type`; now it calculates pseudo-atomic orbitals before and after the optimization. The center table specifies orbitals to be plotted in the left bottom figure; `s0` (2s orbital) is now selected. The right bottom table can show linear combination coefficients or norms of orbitals. Now it shows the contraction coefficients for s orbitals ($l = 0$); the upper ones are from the `Contraction.coefficients` data block and the lower ones are calculated from inner products of orbitals before and after the optimization.

Some errors occurred when files in OpenMX were directly used. `Docs/DFT_DATA19_mod.md` lists necessary modifications to perform calculations.

2.2.4 OpenMX_band

The tool can show band dispersion and LCAO coefficients. It is generated during the development of `Main_GUI/SPADExp_GUI.py`, so users are recommended to use the latter.

2.3 OpenMX_tools directory

The tools included in the `OpenMX_tools` directory are described. They are necessary as the interface with OpenMX.

2.3.1 Compilation

The programs are compiled with the `make` command and a C++ compiler. Users need to install HDF5 [15] before the compilation. **When they install HDF5, they need to set `--enable-cxx` option in the `configure` command.**

Users create `Makefile` referring to `Makefile_example` and specify the path where HDF5 is installed. Then they can compile programs.

2.3.2 preproc.o

`preproc.o` create the input file to calculate LCAO coefficients in OpenMX. It needs two arguments, the paths of the input and output files.

```
> preproc.o (input file) (output file)
```

The input file includes input parameters for OpenMX and keywords in Table 2.3. All keywords are mandantory; the values of `minN` `maxN` are not loaded in `preproc.o` but necessary for `postproc.o`. We recommend to set 0 to `num.HOMOs` and `num.LUMOs`. Three numbers to specify the point in the reciprocal space are fractional coordinates of the reciprocal lattice. The basis set is the reciprocal lattice vectors of `Band.KPath.UnitCell` or `Atom.UnitVectors`. If both unit cell are in the input file, the former is used as the band dispersion calculations do.

Table 2.3: Keywords for `preproc.o`.

Keyword	Value	Description
<code>SPAExp.dimension</code>	Number 1 or 2	Dimension of the reciprocal space
<code>SPAExp.curved</code>	Boolean	Whether the target is curved or flat
<code>SPAExp.origin</code>	Three real numbers	Origin of the target space
<code><SPAExp.range</code> <code>SPAExp.range></code>	Five real numbers, one integer Same numbers of lines as the dimension	Reciprocal space Three in the beginning are for the vector Following two are for the range The last integer is for the number of points
<code>SPAExp.minN</code>	Integer	The lowest band index to be considered
<code>SPAExp.maxN</code>	Integer	The highest band index to be considered

The output file includes the same content as the input and `M0.fileout`, `M0.Nkpoint`, and `M0.kpoint` keywords according to values in Table 2.3. Although keywords in Table 2.3 remain in the output, they cause no error because OpenMX neglects unnecessary keywords.

The reciprocal space is specified by `origin` and `range` as follows. In this explanation, `dimension` is fixed to 1 and \mathbf{a}_i ($i = 1, 2, 3$) represent the bases for the reciprocal lattice.

1. Values of `origin` (o_1, o_2, o_3) determines the origin $\mathbf{o} = \sum_i o_i \mathbf{a}_i$.
2. Values of `range` (x_1, x_2, x_3 , three in the beginning) determines the direction vector $\mathbf{x} = \sum_i x_i \mathbf{a}_i$.
3. It checks that \mathbf{o} and \mathbf{x} are orthogonal.
4. Values of `range` (p_1, p_2, n , three in the end) determines the distance $d = (p_2 - p_1)/(n - 1)$.
5. The i th reciprocal point is

$$\mathbf{v}_i = \mathbf{o} + (p_1 + i \times d)\mathbf{x} \quad (2.1)$$

if `curved` is false (flat plane/straight line) and

$$\mathbf{v}_i = r \cdot \mathbf{o} + (p_1 + i \times d)\mathbf{x} \quad (2.2)$$

if `curved` is true (curved plane/curve). The coefficient r is determined so that $|\mathbf{v}_i| = |\mathbf{o}|$ holds.

2.3.3 postproc.o

`postproc.o` loads the output of OpenMX and generate a HDF5 file. It requires one argument, the path of the input for OpenMX (output of `preproc.o`).

```
> postproc.o (input file)
```

It reads the unit cell, band dispersion, LCAO coefficients and so on from the input file and the output of OpenMX *System.Name.out*. In the output of OpenMX, LCAO coefficients are written in the form of a list like Ref. [16]; the loops to determine the order are atom label, angular quantum number, principal quantum number, and magnetic quantum number, from the outside. Basis sets used in OpenMX are not eigenstate of the magnetic quantum number m but real functions obtained by combining eigenstates of the magnetic quantum number $\pm m$. For the order of the magnetic quantum number, see `source/Band_DFT_M0.c` in the OpenMX source.

2.4 SPADEXP_GUI tools

Tools included in the SPADEXP_GUI directory are described. One is the Python-based photoemission angular distribution (PAD) calculator SPADEXP_GUI.py, and the other is the viewer SPADEXP_Viewer.py.

We recommend to perform calculations on the C++ version if the reciprocal space is two-dimensional or the system is large. The python version does not include the matrix element calculations using the modified plane wave and the weighting, which are included in the C++ version.

2.4.1 SPADEXP_GUI

The tool calculates the photoemission angular distribution from the HDF5 file output from postproc.o. Users need to set the path of PAO_and_AO_after_opt.hdf5 to the variable PAO_and_AO in Config.py. Also, they need to set the path of elements.ini in VESTA [17] to the variable elements_file.

Figure 2.4.1 shows the execution example. The left bottom panel shows the unit cell, and the Boundaries determines the number of repetitions. The straight line in pen_pol represents the angle for the polarization (Θ , Φ). The straight lines in pen_kx and pen_ky represent the directions to specify the calculation region.

The center panel is the band dispersion or the PAD. Each band is stretched according to the gaussian with the width dE to obtain the color map. In case of 2D (dimension is one), green vertical and horizontal lines appear. The right table shows the LCAO coefficients or orbital shape at the crossing point of the cursors. The left and right keys change the k point, and the top and bottom keys change the band index. In case of 3D (dimension is two), the left and the right are for k_x , the top and the bottom are for k_y , Page Up/Page Dn are for the constant-energy map, home/end are for the band index.

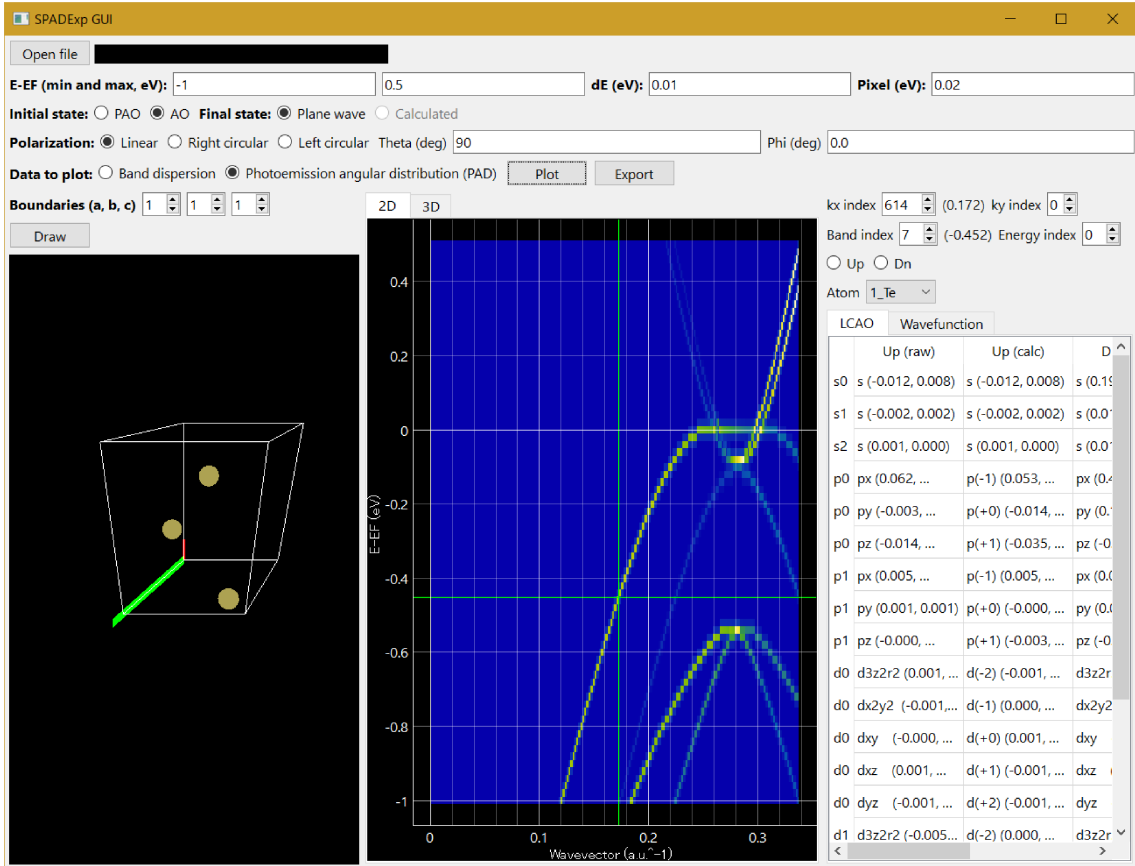


Figure 2.7: Example of SPADEXP_GUI.py.

2.4.2 SPADEXP_Viewer

It displays the PAD in the HDF5 exported by SPADEXP.o or SPADEXP_GUI.py. Figure 2.4.2 shows the example. Users can control the cursors in the 3D case by the same way as SPADEXP_GUI.py. In case of the

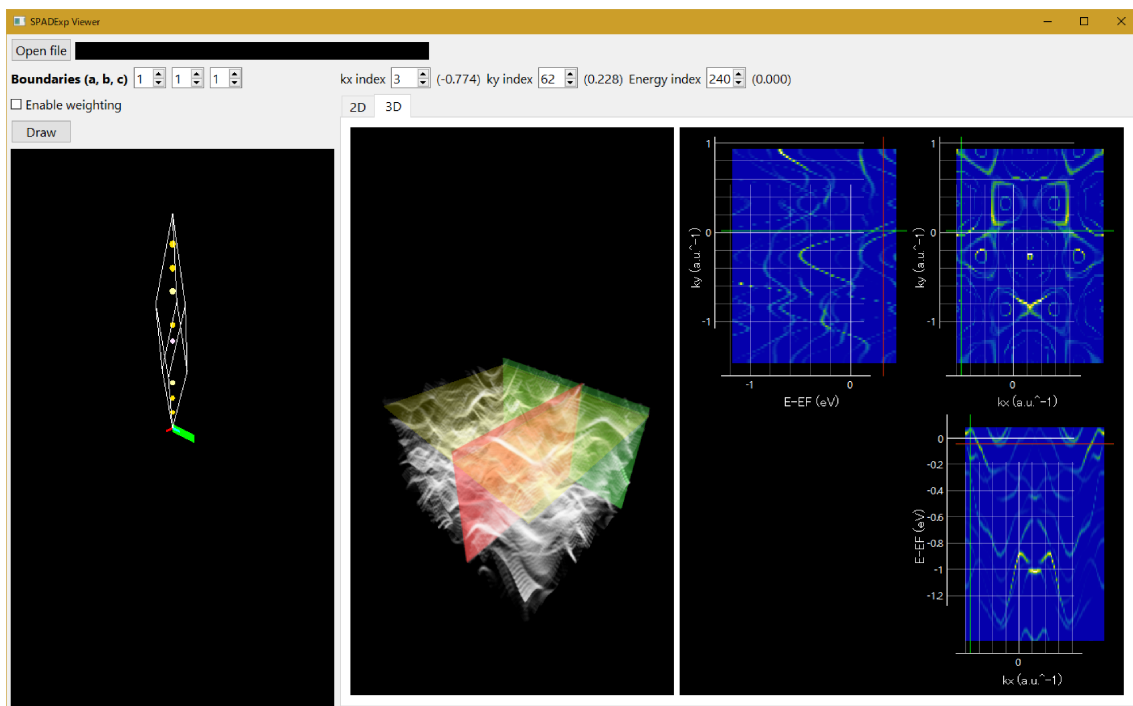


Figure 2.8: Example of SPADEP-Viewer.py.

PAD calculations with the weighting function, `Enable weighting` changes the transparency of atoms according to the weight of them.

2.5 Main_program directory

Tools in `Main_program` directory are described. The executable `SPADExp.o` can calculate atomic potentials and PADs.

2.5.1 Compilation

Similarly to the `OpenMX_tools` directory, users need to make `Makefile` based on `Makefile_example` and compile the program by the `make` command. In addition to HDF5, libraries for the OpenMP parallelization and BLAS, such as Intel MKL, are necessary.

2.5.2 Overview

The successful compilation generates the executable `SPADExp.o`. Users can perform calculations by loading the input file to the standard input.

```
> SPADExp.o < input.dat
```

The input file is a text file with similar format to Quantum ESPRESSO. It contains several blocks, which start with `&block_name` and end with `/`. In a block, each line contains the keyword and the value with spaces between them. Lines starting with `!` or `#` and blank lines are neglected. There is no rule for the order of blocks, while multiple blocks with the same name are forbidden.

The keywords and values are case-sensitive. The values have the following types.

Integer 1

Real number 1.5 or 1.0e-2

Boolean TRUE True true or FALSE False false

String /path/to/file

2.5.3 &Control block

The `&Control` block specifies the calculation type and input and output files. Table 2.4 describes the keyword. Keywords without the default values are generally mandatory; the calculations cannot be executed if the values are given.

Table 2.4: Keywords and values for the `&Control` block.

Keyword	Type	Description	Default
<code>Calculation</code>	String	Calculation type	None
<code>Log_file</code>	String	Path to the log file	None
<code>Console_log</code>	Boolean	Whether the log is output to the console or not	True
<code>Output_file</code>	String	Path to the output file	None

2.5.4 Calculation of the Thomas-Fermi potential

When `Calculation` is set to `Thomas-Fermi`, the software calculates the Thomas-Fermi potential $g(x)$. The differential equation to be solved is

$$\frac{d}{dx^2}g(x) = \frac{g(x)^{3/2}}{\sqrt{x}}. \quad (2.3)$$

See Section 1.2 for the details of the calculation process.

The keywords are specified in the `&Thomas-Fermi` blocks. Table 2.5 shows the keywords. In the test calculation, the software calculates $g(x)$ for given $g'(0)$ values. In the actual calculation, the software finds the solution satisfying $g(x) \rightarrow 0$ ($x \rightarrow \infty$) by the bisection method using the given minimum and maximum of $g'(0)$. The default values for `Initial_diff_min` and `Initial_diff_max` are chosen so that it successfully finds the solution with the 4th-order Runge-Kutta method.

Table 2.5: Keywords and values for the **&Thomas-Fermi** block.

Keyword	Type	Description	Default
Calculation_test	Boolean	Test calculation or actual calculation	False (actual)
Initial_diff_offset	Real number	[Test] the initial value of $g'(0)$	None
Initial_diff_delta	Real number	[Test] increment for $g'(0)$	None
Initial_diff_size	Real number	[Test] number of points for $g'(0)$	None
Initial_diff_min	Real number	[Actual] the initial bottom for $g'(0)$	-1.49
Initial_diff_max	Real number	[Actual] the initial top for $g'(0)$	-1.51
Threshold	Real number	Convergence threshold	1e-5
Solution	String	Method to solve the differential equation RK1(Euler method) RK4(4th-order Runge-Kutta method)	RK4

In the calculations of the Thomas-Fermi potential, the **&Radial-grid** block can specify the sequence of points x_i for the calculations of $g(x_i)$. The number of lines in the block are described in the **&Radial-grid** line. Each line in the block specifies the increment (real number) and the number of points (integer). The default is the same as Ref. [2].

```
&Radial_grid 11
0.0025 40
0.005 40
0.01 40
0.02 40
0.04 40
0.08 40
0.16 40
0.32 40
0.64 40
1.28 40
2.56 40
/
```

2.5.5 Calculations of atomic wave functions

When **Calculation** is set to **Atomic-wfn**, the software calculates the radial wave function in the spherically isotropic atomic potential. See Section 1.2 for the details of the calculations.

The keywords are specified in the **&Atomic-wfn** block, as well as the **&Radial-grid** block for x_i . Table 2.6 shows the keywords. For the principal quantum number, users can specify multiple values by **n_min** and **n_max** or one value by **n**; both ways cannot be used simultaneously. The similar limitation is applied for the angular quantum numbers and the atomic numbers.

The potential is set to $V(x) = -Z/\mu x$ for **H-like** (hydrogen-like atom), $V(x) = -Z/\mu x \cdot g(x)$ for **Thomas-Fermi** ($g(x)$ is given by the file), and the values in the file for **file**. In the above equation, μ is the Thomas-Fermi scaling coefficient.

The output includes eigenvalues for each atom.

Table 2.6: Keywords and values for the `&Atomic-wfn` block.

Keyword	Type	Description	Default
<code>n_min</code>	Integer	Minimum of the principal quantum number n	None
<code>n_max</code>	Integer	Maximum of the principal quantum number n	None
<code>n</code>	Integer	Value of the principal quantum number n	None
<code>l_min</code>	Integer	Minimum of the angular quantum number l	None
<code>l_max</code>	Integer	Maximum of the angular quantum number l	None
<code>l</code>	Integer	Value of the angular quantum number l	None
<code>Z_min</code>	Integer	Minimum of the atomic number Z	None
<code>Z_max</code>	Integer	Maximum of the atomic number Z	None
<code>Z</code>	Integer	Value of the atomic number Z	None
<code>Potential</code>	String	Type of the potential	None
		H-like (hydrogen-like atom)	
		Thomas-Fermi(Thomas-Fermi potential)	
<code>Potential_file</code>	String	file (from file)	None
<code>Solution</code>	String	File containing the potential	None
		Method to solve the differential equation	
		RK1 (Euler method)	
<code>Bisubsection_step</code>	Real number	Numerov (Numerov method)	Numerov
<code>E_threshold</code>	Real number	Initial step size in the bisection method	<code>1e-3</code>
<code>Radius_factor</code>	Real number	Threshold for the energy convergence	<code>1e-5</code>
		Coefficient to determine the calculation range of x	<code>8.0</code>

2.5.6 Calculations of the self-consistent atomic potential

When `Calculation` is set to `SCF-atom`, the software calculates the self-consistent atomic potential. See Section 1.2 for the details of the calculations.

The keywords are specified in the `&SCF-atom`, `&Atomic-wfn`, `&Occupation`, and `&Radial-grid` blocks. Table 2.7 shows the valuable keywords in the `&Atomic-wfn` block. The input potential is used as the initial value for the self-consistent calculations.

Table 2.7: The keywords in the `&Atomic-wfn` block used in the self-consistent calculations.

Keyword	Note
<code>Z</code>	<code>Z_min</code> and <code>Z_max</code> are forbidden
<code>Potential</code>	Set to Thomas-Fermi regardless of the input
<code>Potential_file</code>	
<code>Solution</code>	
<code>Bisubsection_step</code>	
<code>Radius_factor</code>	

Table 2.8 shows the keywords for the `&SCF-atom` block.

Table 2.8: Keywords and values for the `&SCF-atom` block.

Keyword	Type	Value	Default
<code>Mix_weight</code>	Real number	Mixing ratio in the self-consistent calculations	0.5
<code>Criterion_a</code>	Real number	Convergence threshold for α	0.001
<code>Criterion_b</code>	Real number	Convergence threshold for β	0.001

The `&Occupation` block specify the occupation number in the shape of stairs. In case of a carbon atom with two electrons in $1s$, $2s$, and $2p$ orbitals, the input becomes like

```
&Occupation 2
2
2 2
/
```

The output is a HDF5 file containing the self-consistent potential and the atomic number.

2.5.7 Calculations of excited states and phase shifts

When **Calculation** is set to **Phase-shift**, the software calculates excited states and phase shifts with the atomic potential.

The keywords are specified in the **&Phase-shift**, **&Atomic-wfn**, **&Radial-grid**, **&Excitation-energy**, and **&Orbital** blocks. Table 2.9 shows the valuable keywords in the **&Atomic-wfn** block. Users set the path of a HDF5 file, obtained by the self-consistent calculations or given by us as a database, to **Potential_file**. If the file is not specified, the potential becomes the hydrogen potential $V(x) = -1/\mu x$, so the calculations give the Coulomb wave function and the phase difference $\arg \Gamma(l + 1 - i/k)$.

Table 2.9: The keywords in the **&Atomic-wfn** block used in the phase shift calculations.

Keyword	Note
Z	Z_min and Z_max are forbidden
Potential_file	
Solution	

Table 2.10 shows the keywords for the **&Phase-shift** block.

Table 2.10: Keywords and values for the **&Phase-shift** block.

Keyword	Type	Description	Default
Skip_points	Integer	Number of skipped local minimum/maximum points	2
Calc_points	Integer	Number of points used for the phase calculation	5

The **&Orbital** block specifies the angular quantum number and the binding energy of the ground states. For example,

```
&Orbital 1
2p 6.0
/
```

means the $2p$ orbital has the binding energy of 6 eV. The **&Excitation-energy** block specifies the excitation energies;

```
&Excitation-energy 1
21.2
/
```

means the excitation by the helium lamp (21.2 eV).

The default values of the **&Radial-grid** block are inappropriate because they do not have enough number of points for large x . The calculation examples use the following grid.

```
&Radial-grid
0.0025 40
0.005 40
0.01 40000
/
```

The output includes the wave functions for the excited states with $l \pm 1$. The beginning of the output file has comments for the phase shift calculated from local minima and maxima.

2.5.8 Photoemission intensity calculations

When `Calculation` is set to `PAD`, the software calculates the PAD. See Section 1.4 for the details of the calculations.

The `&PAD` block is used. Table 2.11 shows the keywords. The gauss distribution with the width `dE` is introduced to realize smooth distribution from discretized dispersions maybe due to slab calculations. `Final_state_step` is used to reduce the number of k points where the software calculate the atomic potential effect. When `Final_state` is set to `Calc`, the `&Radial-grid` block, `Potential_file` and `Solution` in the `&Atomic-wfn` block, and the `&Phase-shift` block are used.

When users use `Extend`, they need to check that the first and last point are different by the reciprocal vector, and the repetition of the region gives the periodic reciprocal space. Therefore, they cannot use `Extend` if `curved` is set to `true` in `preproc.o`. The software does not check the periodicity. In the one-dimensional case, the second (right) and fourth (left) values are used.

The weighting is applied by the following process. For an atom at \mathbf{r}_i , the software determines the distance z_i by the inner product with the unit vector \mathbf{v} specified by `Weighting_axis`. The following equation gives the weight; if $\lambda > 0$,

$$W_{\text{Rect}}(z_i) = \begin{cases} 1 & z_0 < z_i < z_0 + \lambda \\ 0 & \text{otherwise} \end{cases} \quad (2.4)$$

$$W_{\text{Exp}}(z_i) = \begin{cases} 0 & z_i < z_0 \\ \exp\left(-\frac{z - z_0}{\lambda}\right) & z_i > z_0, \end{cases} \quad (2.5)$$

and if $\lambda < 0$,

$$W_{\text{Rect}}(z_i) = \begin{cases} 1 & z_0 - |\lambda| < z_i < z_0 \\ 0 & \text{otherwise} \end{cases} \quad (2.6)$$

$$W_{\text{Exp}}(z_i) = \begin{cases} 0 & z_i > z_0 \\ \exp\left(\frac{z - z_0}{|\lambda|}\right) & z_i < z_0, \end{cases} \quad (2.7)$$

where z_0 represents `Weighting_origin` and λ represents `Weighting_width` [Fig. 2.9].

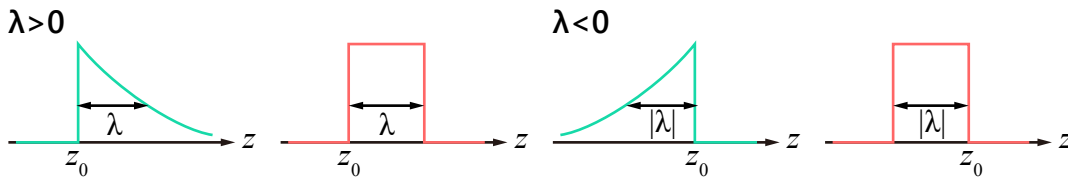


Figure 2.9: Schematic of the weighting functions.

Figure 2.10 shows the polarizations and angles Θ , Φ . Table 2.12 represents the $\mathbf{r} \cdot \mathbf{e}$ term for each polarization.

The output file is a HDF5 file containing the PAD, unit cell, and so on.

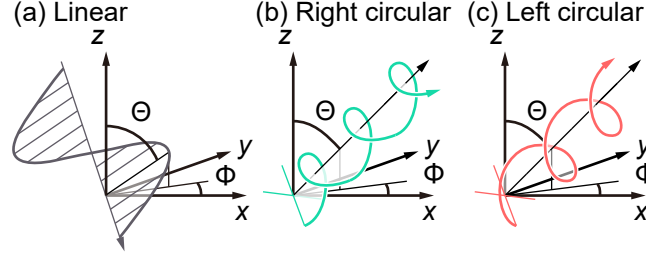
Figure 2.10: Schematic of linear and circular polarizations and angle Θ , Φ .

Table 2.11: Keywords and values for the &PAD block.

Keyword	Type	Description	Default
Input_file	String	File path to the output of postproc.o	None
E_min	Real number	Minimum of the energy range	None
E_max	Real number	Maximum of the energy range	None
E_pixel	Real number	Step along the energy direction	None
dE	Real number	Width of the gaussian	None
Initial_state	String	Initial states AO or PAO	None
Final_state	String	Final states PW (plane wave) Calc (modified plane wave)	None
Final_state_step	Real number	Discretization width for the atomic potential effect calculations	0.01
Polarization	String	Polarization Linear (linear) LCircular (left circular) RCircular (right circular)	None
Theta	Real number	Angle Θ [degree] for the polarization direction	None
Phi	Real number	Angle Φ [degree] for the polarization direction	None
Atomic_orbitals_file	String	Database file for AO and PAOs	None
Extend	4 integers	Extension width for top, right, bottom, and left	Zero
Weighting	Boolean	Whether weighting is applied	False
Weighting_axis	3 real numbers	Axis for the weighting	None
Weighting_shape	String	Shape of the weighting function Rect (rectangular) or Exp (exponential)	None
Weighting_origin	Real number	Origin for the weighting	None
Weighting_width	Real number	Width of the weighting function	None
Use_angstrom	Boolean	Å is used for the unit of Weighting_origin and Weighting_width , or Bohr is used	True
Output_data	String	Output data PAD (normal PAD) Band (the matrix element is fixed to 1)	PAD

Table 2.12: $\mathbf{r} \cdot \mathbf{e}$ terms for linear and circular polarization.

Polarization	\mathbf{e}	$\mathbf{r} \cdot \mathbf{e}$
Linear	$\begin{pmatrix} \sin \theta \cos \varphi \\ \sin \theta \sin \varphi \\ \cos \theta \end{pmatrix}$	$\begin{aligned} & -\sqrt{\frac{2\pi}{3}} \sin \theta e^{-i\varphi} \cdot rY_{1,1} \\ & + \sqrt{\frac{4\pi}{3}} \cos \theta \cdot rY_{1,0} \\ & + \sqrt{\frac{2\pi}{3}} \sin \theta e^{i\varphi} \cdot rY_{1,-1} \end{aligned}$
Right circular	$\begin{pmatrix} -\cos \theta \cos \varphi \\ -\cos \theta \sin \varphi \\ \sin \theta \end{pmatrix} + i \begin{pmatrix} \sin \varphi \\ -\cos \varphi \\ 0 \end{pmatrix}$	$\begin{aligned} & \sqrt{\frac{2\pi}{3}} (1 + \cos \theta) e^{-i\varphi} \cdot rY_{1,1} \\ & + \sqrt{\frac{4\pi}{3}} \sin \theta \cdot rY_{1,0} \\ & + \sqrt{\frac{2\pi}{3}} (1 - \cos \theta) e^{i\varphi} \cdot Y_{1,-1} \end{aligned}$
Left circular	$\begin{pmatrix} -\cos \theta \cos \varphi \\ -\cos \theta \sin \varphi \\ \sin \theta \end{pmatrix} - i \begin{pmatrix} \sin \varphi \\ -\cos \varphi \\ 0 \end{pmatrix}$	$\begin{aligned} & \sqrt{\frac{2\pi}{3}} (-1 + \cos \theta) e^{-i\varphi} \cdot rY_{1,1} \\ & + \sqrt{\frac{4\pi}{3}} \sin \theta \cdot rY_{1,0} \\ & - \sqrt{\frac{2\pi}{3}} (1 + \cos \theta) e^{i\varphi} \cdot Y_{1,-1} \end{aligned}$

Bibliography

- [1] <https://physics.nist.gov/cuu/Constants/index.html>
- [2] Herman and Skillman “Atomic Structure Calculations ”, 1963.
- [3] R. Latter, Phys. Rev. **99**, 510 (1955).
- [4] E. Heirer, S.P. Nørsett, and G. Wanner, “Solving Ordinary Differential Equations I”, Springer, 1993.
- [5] 西森 秀稔、「物理数学 II」、丸善出版、2015。
- [6] NIST Digital Library of Mathematical Functions, <https://dlmf.nist.gov> .
- [7] E. U. Condon and G. H. Shortley, “The Theory of Atomic Spectra”, Cambridge Univ. Press, 1999.
- [8] 猪木 慶治、川合 光、「量子力学 II」、講談社、2007。
- [9] <http://www.openmx-square.org/>
- [10] http://www.openmx-square.org/adpack_man2.2/
- [11] R. M. Martin “Electronic Structure: Basic Theory and Practical Methods”, 2nd edition, Cambridge University Press, 2020.
- [12] T. Ozaki, Phys. Rev. B **67**, 155108 (2003).
- [13] <http://www.openmx-square.org/video-lec/OrderN-Part2.pdf>, pp.4-20.
- [14] http://www.openmx-square.org/adpack_man2.2-jp/node22.html
- [15] <https://www.hdfgroup.org/downloads/hdf5/>
- [16] http://www.openmx-square.org/openmx_man3.8jp/node93.html
- [17] <https://jp-minerals.org/vesta/en/>
- [18] J. A. Sobota, Y. He, and Z. X. Shen, Rev. Mod. Phys. **93**, 025006 (2022).
- [19] T. Matsushita *et al.*, Phys. Rev. B **56**, 7687 (1997).
- [20] S. Moser, J. Electron Spectrosc. **214**, 29 (2017).
- [21] J. Stöhr, and H. C. Siegmann, “Magnetism: From Fundamentals to Nanoscale Dynamics”, Springer, 2007.
- [22] N. H. March, Advances in Physics **6**, 1 (1957).
- [23] G. Breit and H. A. Bethe, Phys. Rev. **93**, 888 (1954).